2023-02-25

# Modeling cryptosporidiosis in humans and cattle: Deterministic and stochastic approache

Luhanda, Faraja

Elsevier

https://doi.org/10.1016/j.parepi.2023.e00293

Parasite Epidemiology and Control 21 (2023) e00293

Contents lists available at ScienceDirect

Parasite Epidemiology and Control

journal homepage: www.elsevier.com/locate/parepi

# Modeling cryptosporidiosis in humans and cattle: Deterministic and stochastic approaches

Faraja Luhanda [a,b,*], Jacob I. Irunde [b], Dmitry Kuznetsov [a]

[a] Department of Applied Mathematics and Computational Science, The Nelson Mandela African Institution of Science and Technology, P.O.Box 447, Tengeru, Arusha, Tanzania

[b] Department Mathematics, Physics and Informatics, University of Dar es Salaam, Mkwawa University College of Education, P.O. Box 2513, Iringa, Tanzania

ARTICLE INFO

*Keywords:*
Cryptosporidiosis
*Cryptosporidium*
Basic reproduction number
Stochastic model
Multitype branching process
Stochastic threshold

ABSTRACT

Cryptosporidiosis is a zoonotic disease caused by *Cryptosporidium*. The disease poses a public and veterinary health problem worldwide. A deterministic model and its corresponding continuous time Markov chain (CTMC) stochastic model are developed and analyzed to investigate cryptosporidiosis transmission dynamics in humans and cattle. The basic reproduction number $\mathbb{R}_0$ for the deterministic model and stochastic threshold for the CTMC stochastic model are computed by the next generation matrix method and multitype branching process, respectively. The normalized forward sensitivity index method is used to determine the sensitivity index for each parameter in $\mathbb{R}_0$. Per capita birth rate of cattle, the rate of cattle to acquire cryptosporidiosis infection from the environment and the rate at which infected cattle shed *Cryptosporidium* oocysts in the environment play an important role in the persistence of the disease whereas *Cryptosporidium* oocysts natural death rate, cattle recovery rate and cattle natural death rate are most negative sensitive parameters in the dynamics of cryptosporidiosis. Numerical results for CTMC stochastic model show that the likelihood of cryptosporidiosis extinction is high when it arises from an infected human. However, there is a major outbreak if cryptosporidiosis emerges either from infected cattle or from *Cryptosporidium* oocysts in the environment or when it emerges from all three infectious compartments. Therefore to control the disease, control measures should focus on maintaining personal and cattle farm hygiene and decontaminating the environment to destroy *Cryptosporidium* oocysts.

## 1. Introduction

Cryptosporidiosis is a zoonotic disease that is caused by *Cryptosporidium*. The disease infects a wide range of hosts including humans and cattle (Pal et al., 2021; Pumipuntu and Piratae, 2018; Thomson et al., 2019), thus it is a serious disease of concern in public and veterinary health (Pumipuntu and Piratae, 2018). In the globe, the disease prevalence varies from 0.1 to 73.3% and 6.25 to 39.65% in humans and cattle respectively (Tarekegn et al., 2021), and it is ranked sixth among prevalent foodborne parasite infections (Pal et al., 2021). Although the disease is self-limiting in immunocompetent humans (Moawad et al., 2021; Rossle and Latif, 2013), it has a high mortality rate in children, the elderly and immunocompromised patients (Rossle and Latif, 2013). Cryptosporidiosis is the second

* Corresponding author at: Department of Applied Mathematics and Computational Science, The Nelson Mandela African Institution of Science and Technology, P.O.Box 447, Tengeru, Arusha, Tanzania.
*E-mail address:* luhandaf@nm-aist.ac.tz (F. Luhanda).

https://doi.org/10.1016/j.parepi.2023.e00293
Received 1 December 2022; Received in revised form 5 February 2023; Accepted 16 February 2023
Available online 25 February 2023

major cause of diarrhea and mortality in children after rotavirus (Striepen, 2013; Zakir et al., 2021) and it is the main cause of morbidity and death in neonatal calves worldwide (Ouakli et al., 2018).

The disease is mainly transmitted through fecal–oral route (Thomson et al., 2019) where humans contract infection through either contact with infected host or ingesting *Cryptosporidium* oocysts from contaminated environment such as contaminated food or water (Pumipuntu and Piratae, 2018; Ramirez et al., 2004). Humans can also acquire the infection through inhalation of *Cryptosporidium* oocysts (Aldeyarbi et al., 2016; Zakir et al., 2021) while cattle acquire the disease through either contact with infected cattle or consuming *Cryptosporidium* oocysts from contaminated environment (Ramirez et al., 2004; Walter et al., 2021). Adult cattle are asymptomatic carriers of the disease (Castro-Hermida et al., 2007; Ibrahim et al., 2016; Nguyen et al., 2007; Scott et al., 1995). In humans, cryptosporidiosis usually causes watery diarrhoea, vomiting, dehydration (Centers for Disease Control and Prevention, 2020), stomach pain, nausea, fever and weight loss in humans (Centers for Disease Control and Prevention, 2020; Desai et al., 2012) and in cattle the disease causes diarrhoea, abdominal pain, weight loss, vomiting and nausea (Gong et al., 2017). Infected cattle are the main contributors of *Cryptosporidium* oocysts into the environment (Hatam-Nahavandi et al., 2019; Mtambo et al., 2000) because an infected calf can shed around $1.1 \times 10^8$ oocysts in a gram of its dung (Hatam-Nahavandi et al., 2019).

Cryptosporidiosis poses a major challenge to humans and cattle health because *Cryptosporidium* oocysts in the environment are resistant to various chemical disinfectants (Rossle and Latif, 2013; Zakir et al., 2021). The world's major outbreak of cryptosporidiosis occurred in 1993 in Milwaukee, Wisconsin in the United States of America, which affected over $400,000$ humans and an economic cost of more than $96.2 million (Zahedi and Ryan, 2020). In the cattle economy, the disease is a critical problem, especially in calves (Hatam-Nahavandi et al., 2019), which causes financial losses due to calf deaths and expenses for diagnosis, supportive services and treatment (Innes et al., 2020). A research by Shaw et al. (2020) depicts that a calf with severe cryptosporidiosis measures 34 kg less on average than an asymptomatic calf. Apart from reducing weights in calves, cryptosporidiosis infection also reduces milk production (Tarekegn et al., 2021; Zakir et al., 2021). Currently, there are no vaccine and effective treatment for cryptosporidiosis (Ikiroma and Pollock, 2021; Innes et al., 2020; Zakir et al., 2021). Therefore, the best preventative measures for humans and cattle are to maintain good personal and cattle farm cleanliness and avoid environmental contamination with *Cryptosporidium* oocysts (Zakir et al., 2021).

Mathematical models are pivotal tools used to investigate and analyze transmission dynamics of infectious diseases for developing effective control strategies. Few deterministic models which include Okosun et al. (2016a), Ogunlade et al. (2016) and Okosun et al. (2017) have been developed and analyzed to study cryptosporidiosis transmission dynamics. Ogunlade et al. (2016) considered optimal control analysis of cryptosporidiosis in humans while Okosun et al. (2017) and Okosun et al. (2016a) focused on dynamics of co-infection of cryptosporidiosis with either HIV-AIDS or Trypanosomiasis respectively. None of the studies have considered cattle population in the transmission dynamics of cryptosporidiosis. Furthermore, no any research has used a Continuous Time Markov Chain (CTMC) stochastic model to investigate dynamics of cryptosporidiosis in humans and cattle. Therefore, this study aims to develop and analyze deterministic and CTMC stochastic models and use a multitype branching process theory to determine the likelihood of disease outbreak or extinction (Allen and Lahodny, 2012; Allen and van den Driessche, 2013).

This paper is organized as follows: formulation of deterministic model and its analysis are presented in Section 2. In Section 3, we formulate and analyze the CTMC stochastic model. Numerical simulations for the models are carried out in Section 4, and the conclusion is presented in Section 5.

## 2. Deterministic model

### 2.1. Model formulation

In formulating the model for cryptosporidiosis dynamics, we modify the work by Ogunlade et al. (2016) by incorporating cattle population. Human and cattle populations $N_H$ and $N_C$ respectively, are divided into susceptible $(S_i)$, infected $(I_i)$ and recovered $(R_i)$ classes. The subscript $i$ takes $H$ for humans and $C$ for cattle.

The susceptible humans $S_H$ increase at a constant per capita birth rate $\Lambda_H$ and acquire the disease through contact with an infected human $I_H$ or infected cattle $I_C$ or through ingesting or inhaling *Cryptosporidium* oocysts $E_V$ at a rate

$$\lambda_H = \psi_H I_H + \psi_C I_C + \psi_E E_V, \tag{1}$$

where $\psi_H, \psi_C$ and $\psi_E$ are the rates of a human to contract infection from infected human, infected cattle and contaminated environment respectively. The infected humans $I_H$ suffer disease induced mortality at a rate $d_H$ and may recover naturally from the disease at a rate $r_H$. The recovered humans $R_H$ lose immunity at a rate $\phi_H$ and return to susceptible class. Natural mortality occurs in all compartments of humans at a rate $\mu_H$.

The susceptible cattle $S_C$ are recruited at a constant per capita birth rate $\Lambda_C$ and contract the disease through contact with infected cattle or ingestion of *Cryptosporidium* oocysts from the environment at a rate

$$\lambda_C = \rho_C I_C + \rho_E E_V. \tag{2}$$

Parameters $\rho_C$ and $\rho_E$ are the rates for cattle to contract infection following contact with infected cattle and intake of *Cryptosporidium* oocysts from a contaminated environment respectively. The infected cattle $I_C$ suffer disease induced mortality at a rate $d_C$ and may recover naturally from the disease at a rate $r_C$. The recovered cattle $R_C$ lose immunity to become susceptible at a rate $\phi_C$. The susceptible and infected cattle are slaughtered at rates $m_1$ and $m_2$ respectively. All cattle compartments suffer natural death at a rate $\mu_C$. The infected humans and cattle shed *Cryptosporidium* oocysts $E_V$ into the environment at rates $\beta_H$ and $\beta_C$ respectively. The

**Table 1**
State variables and their descriptions.

| Variable | Description |
|---|---|
| $S_H$ | Susceptible humans |
| $I_H$ | Infected humans |
| $R_H$ | Recovered humans |
| $S_C$ | Susceptible cattle |
| $I_C$ | Infected cattle |
| $R_C$ | Recovered cattle |
| $E_V$ | *Cryptosporidium* oocysts population in the environment |

**Table 2**
Model parameters and their descriptions.

| Parameter | Description |
|---|---|
| $\Lambda_H$ | Per capita birth rate for humans |
| $\psi_H$ | Rate of a human to acquire infection from infected human |
| $\psi_C$ | Rate of a human to acquire infection from infected cattle |
| $\psi_E$ | Rate of a human to acquire infection from contaminated environment |
| $\mu_H$ | Humans natural mortality rate |
| $d_H$ | Cryptosporidiosis induced mortality in humans |
| $r_H$ | Recovery rate of humans |
| $\phi_H$ | Human rate of lose immunity and return to susceptible class |
| $\Lambda_C$ | Per capita birth rate for cattle |
| $\rho_C$ | Rate of a cattle to acquire infection from infected cattle |
| $\rho_E$ | Rate of a cattle to acquire infection from contaminated environment |
| $\mu_C$ | Cattle natural death rate |
| $d_C$ | Cryptosporidiosis induced death in cattle |
| $m_1$ | Slaughter rate of susceptible cattle |
| $m_2$ | Slaughter rate of infected cattle |
| $r_C$ | Recovery rate of cattle |
| $\phi_C$ | Cattle rate of lose immunity and return to susceptible class |
| $\beta_H$ | Rate of shedding *Cryptosporidium* oocysts by infected human in the environment |
| $\beta_C$ | Rate of shedding *Cryptosporidium* oocysts by infected cattle in the environment |
| $\mu_E$ | *Cryptosporidium* oocysts natural death rate |

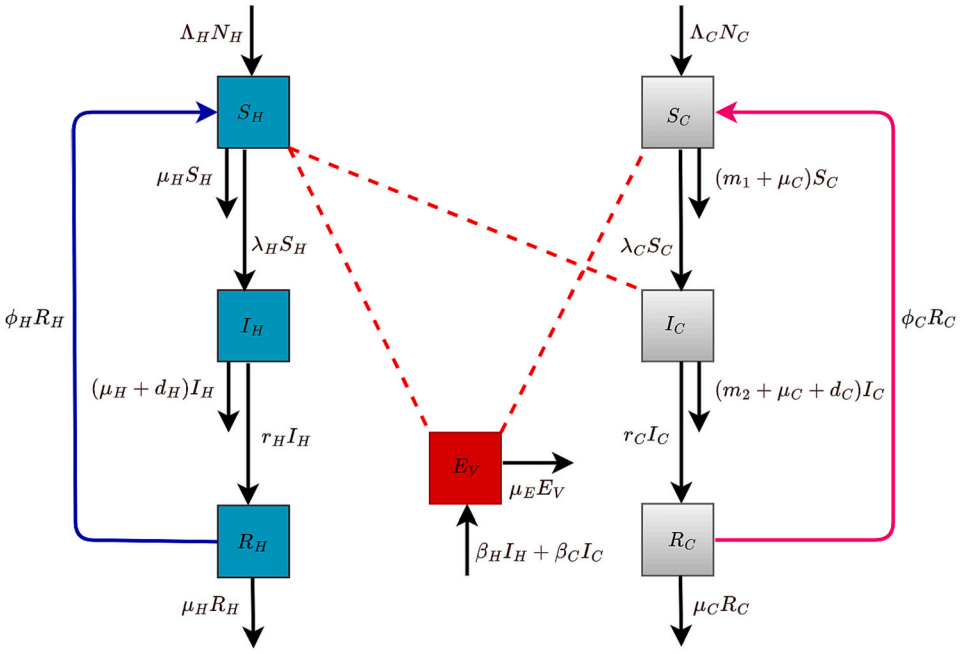


**Fig. 1.** Compartmental diagram for the transmission of cryptosporidiosis. Solid arrows depict the transfer of host from one compartment to another, whereas dashed lines indicate the interactions that cause infections.

*Cryptosporidium* oocysts $E_V$ decrease as a result of the natural death rate $\mu_E$.

We assume that: there is interaction between humans and cattle and all are susceptible to disease. The overall number of *Cryptosporidium* oocysts in the environment is not significantly affected by the number that is consumed to cause infection in humans and cattle. The incubation period of the disease is not considered (Ogunlade et al., 2016; Okosun et al., 2016, 2017). The infected human may recover from the disease naturally without treatment (Ogunlade et al., 2016; Ryan et al., 2016; Sponseller et al., 2014; Sulżyc-Bielicka et al., 2018; Tomczak et al., 2022). Adult cattle are carriers of the disease (Castro-Hermida et al., 2007; Ibrahim et al., 2016; Nguyen et al., 2007; Scott et al., 1995) and infected calves may recover from the disease naturally (Lombardelli et al., 2019; Robertson et al., 2014; Shahiduzzaman and Daugschies, 2012; Siddique et al., 2021). The recovered humans and cattle acquire temporary immunity to the disease.

Tables 1 and 2 describe the state variables and model parameters respectively while Fig. 1 shows the interactions between humans, cattle and *Cryptosporidium* oocysts in the environment.

Thus the transmission dynamics of cryptosporidiosis in humans and cattle is given by the following system:

$$\begin{aligned}
\frac{dS_H}{dt} &= \Lambda_H N_H + \phi_H R_H - (\lambda_H + \mu_H) S_H, \\
\frac{dI_H}{dt} &= \lambda_H S_H - (\mu_H + d_H + r_H) I_H, \\
\frac{dR_H}{dt} &= r_H I_H - (\mu_H + \phi_H) R_H, \\
\frac{dS_C}{dt} &= \Lambda_C N_C + \phi_C R_C - (m_1 + \lambda_C + \mu_C) S_C, \\
\frac{dI_C}{dt} &= \lambda_C S_C - (m_2 + d_C + \mu_C + r_C) I_C, \\
\frac{dR_C}{dt} &= r_C I_C - (\mu_C + \phi_C) R_C, \\
\frac{dE_V}{dt} &= \beta_H I_H + \beta_C I_C - \mu_E E_V, \\
N_H(t) &= S_H(t) + I_H(t) + R_H(t), \\
N_C(t) &= S_C(t) + I_C(t) + R_C(t),
\end{aligned} \tag{3}$$

with initial conditions:

$S_H(0) > 0; I_H(0) \geqslant 0; R_H(0) \geqslant 0; S_C(0) > 0; I_C(0) \geqslant 0; R_C(0)$ and $E_V(0) \geqslant 0$.

### 2.2. Positivity of solutions and invariant region

If the solutions to the model system (3) are non-negative and bounded, then the system is meaningful.

#### 2.2.1. Positivity of solutions

Let us consider the susceptible human equation in the model system (3) which is written as

$$\begin{aligned}
\frac{dS_H}{dt} &= \Lambda_H N_H + \phi_H R_H - (\in \lambda_h + \mu_h) S_H, \text{ then} \\
\frac{dS_H}{dt} &\geqslant -(\lambda_H + \mu_H) S_H \text{ (for } N_H > 0 \text{ and } R_H \geqslant 0), \\
\frac{dS_H}{S_H} &\geqslant -(\lambda_H + \mu_H) dt, \\
S_H(t) &\geqslant S_H(0) e^{-\int_0^t (\lambda_H + \mu_H) d\tau} \geqslant 0, \quad \forall t \geqslant 0.
\end{aligned} \tag{4}$$

Likewise, it can be shown that

$$I_H(t) \geqslant 0; R_H(t) \geqslant 0; S_C(t) \geqslant 0; I_C(t) \geqslant 0; R_C(t) \geqslant 0; E_V(t) \geqslant 0; \forall t \geqslant 0.$$

Thus, $\forall t \geqslant 0$, all solutions of the model system (3) are non-negative.

#### 2.2.2. Invariant region

To test the well-posedness of the model system epidemiologically and mathematically, we investigate the feasibility of its solutions. The model system (3) can be written in the form:

$$\frac{dZ}{dt} = M(Z)Z + K$$

where $Z = (S_H, I_H, R_H, S_C, I_C, R_C, E_V)^T$,

$$M(Z) = \begin{pmatrix} -(\lambda_H + \mu_H) & 0 & \phi_H & 0 & 0 & 0 & 0 \\ \lambda_H & -(\mu_H + d_H + r_H) & 0 & 0 & 0 & 0 & 0 \\ 0 & r_H & -(\mu_H + \phi_H) & 0 & 0 & 0 & 0 \\ 0 & 0 & 0 & -m_{11} & 0 & \phi_C & 0 \\ 0 & 0 & 0 & \lambda_C & -m_{22} & 0 & 0 \\ 0 & 0 & 0 & 0 & r_C & -(\mu_C + \phi_C) & 0 \\ 0 & \beta_H & 0 & 0 & \beta_C & 0 & -\mu_E \end{pmatrix}$$

with $m_{11} = (m_1 + \lambda_C + \mu_C), m_{22} = (m_2 + d_C + \mu_C + r_C)$, and $K = (\Lambda_H N_H, 0, 0, \Lambda_C N_C, 0, 0, 0)^T$.

It is clear that $M(Z)$ is a Metzler matrix because it has all non-negative off-diagonal elements $\forall Z \in \mathbb{R}^7_+$. Since $K \geqslant 0$, the model system (3) is positively invariant in $\mathbb{R}^7_+$ which implies that the solutions of the model system (3) start and remain in $\mathbb{R}^7_+$. Moreover, $K$ is Lipschitz continuous. Hence the feasible region $\Omega$ for the model system (3) is $\Omega = \{(S_H, I_H, R_H, S_C, I_C, R_C, E_V) \geqslant 0\} \in \mathbb{R}^7_+$. Therefore, the model system (3) is well-posed epidemiologically and mathematically in the region $\Omega$. It is thus enough to examine the dynamics of the model system (3) in $\Omega$.

### 2.3. Steady states and basic reproduction number $\mathbb{R}_0$

#### 2.3.1. The disease free equilibrium $(\mathbb{T}^0)$

If there is no cryptosporidiosis in humans and cattle, the disease free equilibrium (DFE) is given by

$$\mathbb{T}^0(S_H^0, I_H^0, R_H^0, S_C^0, I_C^0, R_C^0, E_V^0) = \left(\frac{\Lambda_H N_H^0}{\mu_H}, 0, 0, \frac{\Lambda_C N_C^0}{m_1 + \mu_C}, 0, 0, 0\right). \tag{5}$$

We use the DFE to compute the basic reproduction number $\mathbb{R}_0$ in the next section.

#### 2.3.2. The basic reproduction number $\mathbb{R}_0$

The basic reproduction number $\mathbb{R}_0$ is the average number of secondary infections caused by an infected individual when introduced into an entirely susceptible population. The disease vanishes in the population when $\mathbb{R}_0 < 1$ and persists when $\mathbb{R}_0 > 1$ (Diekmann et al., 1990). The basic reproduction number $\mathbb{R}_0$ which governs the dynamics of cryptosporidiosis is computed by the next-generation matrix approach as derived by Van den Driessche and Watmough (2002). Let $\mathbb{F}_j$ and $\mathbb{V}_j$ be the new infections and the transition terms in infected class $j$ respectively. From the model system (3), we have

$$\mathbb{F}_j = \begin{pmatrix} (\psi_H I_H + \psi_C I_C + \psi_E E_V) S_H \\ (\rho_C I_C + \rho_E E_V) S_C \\ 0 \end{pmatrix}, \mathbb{V}_j = \begin{pmatrix} (\mu_H + d_H + r_H) I_H \\ (\mu_C + d_C + r_C + m_2) I_C \\ \mu_E E_V - \beta_H I_H - \beta_C I_C \end{pmatrix}. \tag{6}$$

The basic reproduction number $\mathbb{R}_0$ is given by

$$\mathbb{R}_0 = \rho(FV^{-1}), \tag{7}$$

where

$$F = \frac{\partial \mathbb{F}_j}{\partial y_i}(\mathbb{T}^0) \text{ and } V = \frac{\partial \mathbb{V}_j}{\partial y_i}(\mathbb{T}^0). \tag{8}$$

Using Eqs. (8), the matrices $F$ and $V$ are given by

$$F = \begin{pmatrix} \frac{\psi_H \Lambda_H N_H^0}{\mu_H} & \frac{\psi_C \Lambda_H N_H^0}{\mu_H} & \frac{\psi_E \Lambda_H N_H^0}{\mu_H} \\ 0 & \frac{\rho_C \Lambda_C N_C^0}{m_1 + \mu_C} & \frac{\rho_E \Lambda_C N_C^0}{m_1 + \mu_C} \\ 0 & 0 & 0 \end{pmatrix} \text{ and}$$

$$V = \begin{pmatrix} (\mu_H + d_H + r_H) & 0 & 0 \\ 0 & (m_2 + d_C + \mu_C + r_C) & 0 \\ -\beta_H & -\beta_C & \mu_E \end{pmatrix}.$$

**Table 3**
Sensitivity indices of $\mathbb{R}_0$ with respect to the parameters.

| Parameter | Sensitivity Index | Parameter | Sensitivity Index |
|---|---|---|---|
| $\Lambda_C$ | +0.899119 | $\mu_E$ | −0.967306 |
| $\rho_E$ | +0.873622 | $r_C$ | −0.882359 |
| $\beta_C$ | +0.873255 | $\mu_C$ | −0.528725 |
| $\Lambda_H$ | +0.100881 | $m_1$ | −0.382539 |
| $\beta_H$ | +0.094051 | $\mu_H$ | −0.100935 |
| $\psi_E$ | +0.093684 | $r_H$ | −0.100785 |
| $\rho_C$ | +0.025497 | $d_C$ | −0.002804 |
| $\psi_H$ | +0.006829 | $m_2$ | −0.001812 |
| $\psi_C$ | +0.000367 | $d_H$ | −0.000041 |

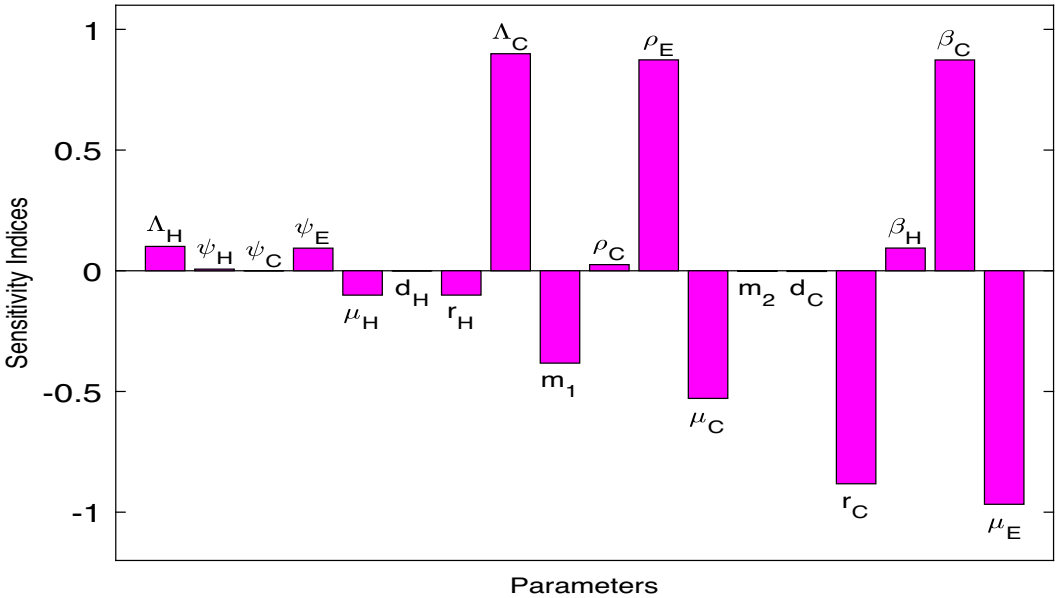


**Fig. 2.** Sensitivity analysis of $\mathbb{R}_0$ with respect to model parameters.

From Eq. (7), the basic reproduction number $\mathbb{R}_0$ is

$$\mathbb{R}_0 = \frac{1}{2}\left(\mathbb{R}_{CE} + \mathbb{R}_{HE} + \sqrt{(\mathbb{R}_{CE} + \mathbb{R}_{HE})^2 + 4\mathbb{R}_{CHE}}\right), \tag{9}$$

where

$$\begin{aligned}
\mathbb{R}_{CE} &= \left(\rho_C + \frac{\beta_C}{\mu_E}\rho_E\right)\frac{1}{(m_2 + d_C + \mu_C + r_C)}\frac{\Lambda_C N_C^0}{(m_1 + \mu_C)},\\
\mathbb{R}_{HE} &= \left(\psi_H + \frac{\beta_H}{\mu_E}\psi_E\right)\frac{1}{(\mu_H + d_H + r_H)}\frac{\Lambda_H N_H^0}{\mu_H},\\
\mathbb{R}_{CHE} &= \frac{(\beta_H(\rho_E\psi_C - \rho_C\psi_E) - \psi_H(\mu_E\rho_C + \beta_C\rho_E))\Lambda_C N_C^0 \Lambda_H N_H^0}{(\mu_H + d_H + r_H)(m_2 + d_C + \mu_C + r_C)(m_1 + \mu_C)\mu_H}\frac{1}{\mu_E}.
\end{aligned} \tag{10}$$

$\mathbb{R}_{CE}$, $\mathbb{R}_{HE}$ and $\mathbb{R}_{CHE}$ represent partial reproduction numbers due to the interaction of cattle and environment, humans and environment, and cattle, humans and environment, respectively.

The terms in (10) can be expounded as follows; $\beta_C/\mu_E$ and $\beta_H/\mu_E$ are the densities of *Cryptosporidium* oocysts shed by infected cattle

and infected humans, respectively. The terms $1/(\mu_H+d_H+r_H)$ and $1/(m_2+d_C+\mu_C+r_C)$ are the average contagious period for human and cattle, respectively; $\Lambda_H N_H^0/\mu_H$ and $\Lambda_C N_C^0/(m_1+\mu_C)$ are initial populations for susceptible humans and cattle, respectively while $1/\mu_E$ is the life expectancy for *Cryptosporidium* oocysts. Parameters which are sensitive to cryptosporidiosis are determined by sensitivity analysis in the following section.

### 2.4. Sensitivity analysis

The normalized forward sensitivity index in Chitnis et al. (2008) is adopted to determine sensitive parameters. Let $\eta_i$ be a parameter in $\mathbb{R}_0$. Its sensitivity index is defined by

$$\Gamma_{\eta_i}^{\mathbb{R}_0} = \frac{\partial \mathbb{R}_0}{\partial \eta_i} \times \frac{\eta_i}{\mathbb{R}_0}. \tag{11}$$

The sensitivity indices of parameters in the $\mathbb{R}_0$ are summarized in Table 3. The positive sign denotes that the increase (or decrease) of the parameter value while other parameters are held fixed, increases (or decreases) the $\mathbb{R}_0$. On the other hand, the negative sign implies that the increase (or decrease) of the parameter value, decreases (or increases) the $\mathbb{R}_0$.

The most positive sensitive parameter is per capita birth rate for cattle $\Lambda_C$ while the most negative sensitive parameter is *Cryptosporidium* oocysts natural death rate $\mu_E$. To eradicate the disease, control and preventive measures should focus on eliminating *Cryptosporidium* oocysts from the environment and practice personal and farm hygiene. Fig. 2 indicates the sensitivity indices for parameters in the $\mathbb{R}_0$.

### 2.5. The endemic equilibrium ($\mathbb{T}^*$)

When cryptosporidiosis persists in humans and cattle, the model system (3) has endemic equilibrium $\mathbb{T}^* = (S_H^*, I_H^*, R_H^*, S_C^*, I_C^*, R_C^*, E_V^*)$. To obtain the endemic equilibrium, we solve for the state variables when the derivatives of model system (3) are zero. In terms of $\lambda_C^*$, the endemic equilibrium is

$$S_C^* = \frac{m\Lambda_C N_C^* + r_C\phi_C I_C^*}{m(\lambda_C^* + z)},\quad I_C^* = \frac{m\Lambda_C N_C^* \lambda_C^*}{bmz + (bm - r_C\phi_C)\lambda_C^*},\quad R_C^* = \frac{r_C I_C^*}{m},$$

$$E_V^* = \frac{mb\beta_H I_H^*(z+\lambda_C^*) + (m\beta_C\Lambda_C N_C^* - r_C\phi_C\beta_H I_H^*)\lambda_C^*}{\mu_E\left(bmz + (bm - r_C\phi_C)\lambda_C^*\right)},$$

$$I_H^* = \frac{\mu_E\lambda_H^*\left(bmz + (bm - r_C\phi_C)\lambda_C^*\right) - m\Lambda_C N_C^*(\beta_C\psi_E + \psi_C\mu_E)\lambda_C^*}{(\psi_E\beta_H + \mu_E\psi_H)\left(bmz + (bm - r_C\phi_C)\lambda_C^*\right)},$$

$$R_H^* = \frac{r_H\left(\mu_E\lambda_H^*\left(bmz + (bm - r_C\phi_C)\lambda_C^*\right) - m\Lambda_C N_C^*(\beta_C\psi_E + \psi_C\mu_E)\lambda_C^*\right)}{A_1},$$

$$S_H^* = \frac{A_1\Lambda_H N_H^* + r_H\phi_H\left(\mu_E\lambda_H^*\left(bmz + (bm - r_C\phi_C)\lambda_C^*\right) - m\Lambda_C N_C^*(\beta_C\psi_e + \psi_C\mu_E)\lambda_C^*\right)}{(\lambda_H^* + \mu_H)A_1},$$

$$\lambda_H^* = \frac{\left(\left(bmz + (bm - r_C\phi_C)\lambda_C^*\right)(\psi_E\beta_H + \mu_E\psi_H) + m\Lambda_C N_C^*(\beta_H(\rho_E\psi_C - \rho_C\psi_E) - A_2\right)\lambda_C^*}{\beta_H\rho_E\left(bmz + (bm - r_C\phi_C)\lambda_C^*\right)}$$

where

$a = (\mu_H + d_H + r_H), b = (m_2 + d_C + \mu_C + r_C), m = (\mu_C + \phi_C), y = (\mu_H + \phi_H), z = (m_1 + \mu_C), A_1 = y(\psi_E\beta_H + \mu_E\psi_H)\left(bmz + (bm - r_C\phi_C)\lambda_C^*\right)$ and $A_2 = \psi_H(\mu_E\rho_C + \beta_C\rho_E)$.

On substituting $S_H^*, I_H^*$ and $\lambda_H^*$ in infected human equation in the model system (3) at steady state, we obtain a fourth degree polynomial whose solutions are $\lambda_C^* = 0$ (which corresponds to the disease free equilibrium) and

$$\lambda_C^{*3} + \Delta_1\lambda_C^{*2} + \Delta_2\lambda_C^* + \Delta_3 = 0 \tag{12}$$

where

$$
\begin{aligned}
\Delta_1 &= A_3 - A_4,\ \ \Delta_2 = A_5 + A_6 + A_7 + A_8,\\
\Delta_3 &= \frac{bm^2 yz\beta_H\rho_E(A_9 - A_{10})}{\mu_E(r_H\phi_H - ay)(r_C\phi_C - bm)^2(\beta_H\psi_E + \mu_E\psi_H)},\\
A_3 &= \frac{y\beta_H\Lambda_H N_H^*\rho_E}{\mu_E(r_H\phi_H - ay)} + \frac{m\Lambda_C N_C^*(\mu_E\rho_C + \beta_C\rho_E)}{(r_c\phi_C - bm)}\left(\frac{1}{\mu_E} + \frac{\psi_H}{(\beta_H\psi_E + \mu_E\psi_H)}\right),\\
A_4 &= \frac{ay\beta_H\mu_H\rho_E}{(r_H\phi_H - ay)(\beta_H\psi_E + \mu_E\psi_H)} + \frac{m}{(r_c\phi_C - bm)}\left(2bz + \frac{\beta_H\Lambda_C N_C^*\rho_E\psi_C}{(\beta_H\psi_E + \mu_E\psi_H)}\right),\\
A_5 &= m^2\left(\left(\frac{(bz - \rho_C\Lambda_C N_C^*)}{(r_C\phi_C - bm)}\right)^2 + \frac{\beta_C\Lambda_C^2 N_C^{*2}\rho_E^2(\beta_C\psi_H - \beta_H\psi_C)}{\mu_E(r_C\phi_C - bm)^2(\beta_H\psi_E + \mu_E\psi_H)}\right),\\
A_6 &= \frac{m^2\rho_E\Lambda_C N_C^*(bz - \rho_C\Lambda_C N_C^*)(\mu_E(\beta_H\psi_C - 2\beta_C\psi_H) + \beta_C\beta_H\psi_E)}{\mu_E(r_C\phi_C - bm)^2(\beta_H\psi_E + \mu_E\psi_H)},\\
A_7 &= \frac{my\beta_H\rho_E\left(\mu_E(2bz - \rho_C\Lambda_C N_C^*)(a\mu_H - \psi_H\Lambda_H N_H^*) - a\beta_C\mu_H\rho_E\Lambda_C N_C^*\right)}{\mu_E(r_H\phi_H - ay)(r_C\phi_C - bm)(\beta_H\psi_E + \mu_E\psi_H)},\\
A_8 &= \frac{my\beta_H\rho_E\Lambda_H N_H^*\left(\rho_E\psi_H\beta_C\Lambda_C N_C^* - \beta_H((2bz - \rho_C\Lambda_C N_C^*)\psi_E + \rho_E\psi_C\Lambda_C N_C^*)\right)}{\mu_E(r_H\phi_H - ay)(r_C\phi_C - bm)(\beta_H\psi_E + \mu_E\psi_H)},\\
A_9 &= (\beta_C + \mu_E)a\mu_H\rho_C\Lambda_C N_C^* + ((\beta_H\psi_E + \mu_E\psi_H)bz + \beta_H\rho_E\psi_C\Lambda_C N_C^*)\Lambda_H N_H^*,\\
A_{10} &= abz\mu_E\mu_H + ((\beta_H\psi_E + \mu_E\psi_H)\rho_C + \beta_C\rho_E\psi_H)\Lambda_C N_C^*\Lambda_H N_H^*.
\end{aligned}
$$

Eq. (12) represents the existence of at most three possible endemic equilibrium points (Kahuru et al., 2017). Thus, there is a chance of the model system (3) to exhibit backward bifurcation when $\mathbb{R}_0 = 1$.

### 2.6. Bifurcation analysis

To explore the possibility of the model system (3) to exhibit backward bifurcation, let the state variables be $S_H = x_1, I_H = x_2, R_H = x_3, S_C = x_4, I_C = x_5, R_C = x_6$ and $E_V = x_7$, so that $N_H = x_1 + x_2 + x_3$ and $N_C = x_4 + x_5 + x_6$, and $a, b, m, y, z$ are given in Section 2.5. In vector form, the state variables are denoted by $X = (x_1, x_2, x_3, x_4, x_5, x_6, x_7)^T$ and the model system (3) can be rewritten in the form $dX/dt = F(X)$ with $F = (f_1, f_2, f_3, f_4, f_5, f_6, f_7)^T$. Thus

$$
\begin{aligned}
\frac{dx_1}{dt} &= f_1 = \Lambda_H(x_1 + x_2 + x_3) + \phi_H x_3 - (\psi_H x_2 + \psi_C x_5 + \psi_E x_7 + \mu_H)x_1,\\
\frac{dx_2}{dt} &= f_2 = (\psi_H x_2 + \psi_C x_5 + \psi_E x_7)x_1 - ax_2,\\
\frac{dx_3}{dt} &= f_3 = r_H x_2 - yx_3,\\
\frac{dx_4}{dt} &= f_4 = \Lambda_C(x_4 + x_5 + x_6) + \phi_C x_6 - (z + \rho_C x_5 + \rho_E x_7)x_4,\\
\frac{dx_5}{dt} &= f_5 = (\rho_C x_5 + \rho_E x_7)x_4 - bx_5,\\
\frac{dx_6}{dt} &= f_6 = r_C x_5 - mx_6,\\
\frac{dx_7}{dt} &= f_7 = \beta_H x_2 + \beta_C x_5 - \mu_E x_7.
\end{aligned}
\tag{13}
$$

The Jacobian matrix of system (13) at the DFE is

$$
J = \begin{pmatrix}
\Lambda_H - \mu_H & \Lambda_H - b_1 & \phi_1 & 0 & -b_2 & 0 & -b_3\\
0 & -(a - b_1) & 0 & 0 & b_2 & 0 & b_3\\
0 & r_H & -y & 0 & 0 & 0 & 0\\
0 & 0 & 0 & \Lambda_C - z & \Lambda_C - d_1 & \phi_2 & -d_2\\
0 & 0 & 0 & 0 & -(b - d_1) & 0 & d_2\\
0 & 0 & 0 & 0 & r_C & -m & 0\\
0 & \beta_H & 0 & 0 & \beta_C & 0 & -\mu_E
\end{pmatrix},
\tag{14}
$$

where $b_1 = \psi_H\Lambda_H N_H^0/\mu_H, b_2 = \psi_C\Lambda_H N_H^0/\mu_H, b_3 = \psi_E\Lambda_H N_H^0/\mu_H, d_1 = \rho_C\Lambda_C N_C^0/z, \quad d_2 = \rho_E\Lambda_C N_C^0/z, \phi_1 = \Lambda_H + \phi_H$ and $\phi_2 = \Lambda_C + \phi_C$.

To investigate whether the system (13) exhibits a backward bifurcation at $\mathbb{R}_0 = 1$, we restate and employ the Theorem 4.1 by Castillo-Chavez and Song (2004) as follows:

**Theorem 1.** *Consider the following general system of ordinary differential equations with a parameter-* $\rho_E : \frac{dx}{dt} = f(x, \rho_E), f : \mathbb{R}^n \times \mathbb{R} \to \mathbb{R}^n$ *and* $f \in \mathbb{C}^2(\mathbb{R}^n \times \mathbb{R})$*, where 0 is an equilibrium point of the system; that is,* $f(0, \rho_E) \equiv 0 \forall \rho_E$ *and*

*1:*$A = D_x f(0,0) = \left(\frac{\partial f_i}{\partial x_j}(0,0)\right)$ *is the linearization matrix of the system around the equilibrium 0 with matrix A evaluated at 0;*

*2:Zero is a simple eigenvalue of A and all other eigenvalues of A have negative real parts;*
*3:Matrix A has a right eigenvector w and a left eigenvector v corresponding to the zero eigenvalue.*

Let $f_k$ be the $k^{th}$ component of $f$ and

$$c_1 = \sum_{k,i,j=1}^{n} v_k w_i w_j \frac{\partial^2 f_k}{\partial x_i \partial x_j}(0,0), \tag{15}$$

$$c_2 = \sum_{k,i=1}^{n} v_k w_i \frac{\partial^2 f_k}{\partial x_i \partial \rho_E}(0,0). \tag{16}$$

The signs of $c_1$ and $c_2$ totally determine the local dynamics of the system (13) around the equilibrium point 0 as follows:

(i).$c_1 > 0$ and $c_2 > 0$. When $\rho_E < 0$ with $|\rho_E| \ll 1, 0$ is locally asymptotically stable, and there exists a positive unstable equilibrium; when $0 < \rho_E \ll 1, 0$ is unstable and there exists a negative and locally asymptotically stable equilibrium;
(ii).$c_1 < 0$ and $c_2 < 0$. When $\rho_E < 0$ with $|\rho_E| \ll 1, 0$ is unstable; when $0 < \rho_E \ll 1, 0$ is locally asymptotically stable, and there exists a positive unstable equilibrium;
(iii).$c_1 > 0$ and $c_2 < 0$. When $\rho_E < 0$ with $|\rho_E| \ll 1, 0$ is unstable, and there exists a locally asymptotically stable negative equilibrium; when $0 < \rho_E \ll 1, 0$ is stable, and a positive unstable equilibrium appears;
(iv).$c_1 < 0$ and $c_2 > 0$. When $\rho_E$ changes from negative to positive, 0 changes its stability from stable to unstable. Correspondingly a negative unstable equilibrium becomes positive and locally asymptotically stable.

Particularly, if $c_1 > 0$ and $c_2 > 0$, then a backward bifurcation occurs at $\rho_E = 0$.

Let $\rho_E = \rho_E^*$ be a bifurcation parameter at $\mathbb{R}_0 = 1$. Calculating for $\rho_E = \rho_E^*$ provided that $\mathbb{R}_0 = 1$, we have

$$\rho_E = \rho_E^* = \frac{(bz - \rho_C \Lambda_C N_C^0)(a\mu_E\mu_H - (\beta_H\psi_E + \mu_E\psi_H)\Lambda_H N_H^0)}{a\mu_H\beta_C\Lambda_C N_C^0 + (\beta_H\psi_C - \beta_C\psi_H)\Lambda_C N_C^0 \Lambda_H N_H^0}. \tag{17}$$

The right eigenvectors $w = (w_1, w_2, \ldots, w_7)^T$ of the Jacobian matrix $J$ are given by

$$w_1 = \frac{b_2 w_5 + b_3 w_7 - ((\Lambda_H - b_1)w_2 + \phi_1 w_3)}{\Lambda_H - \mu_H}, w_2 = \frac{(b - d_1)\mu_E - d_2\beta_C}{(b - d_1)\beta_H} w_7,$$
$$w_3 = \frac{r_H}{y} w_2, w_4 = \frac{d_2(m(b_1 - \Lambda_C) - r_c\phi_2)}{m(b - d_1)(\Lambda_C - z)} w_7, w_5 = \frac{d_2}{b - d_1} w_7, w_6 = \frac{d_2 r_c}{m(b - d_1)} w_7,$$
$$w_7 > 0 \text{ isfree.}$$

The Jacobian matrix $J$ also has left eigenvectors $v = (v_1, v_2, \ldots, v_7)^T$, given by

$$v_1 = v_3 = v_4 = v_6 = 0, v_2 = \frac{\beta_H}{a - b_1} v_7, v_5 = \frac{b_2\beta_H + \beta_C(a - b_1)}{(a - b_1)(b - d_1)} v_7, v_7 > 0 \text{ isfree.}$$

*2.6.1. Computations of $c_1$ and $c_2$ from Eqs. (15) and (16)*

Since $v_1 = v_3 = v_4 = v_6 = 0$, that is, $k = 1, 3, 4, 6$, then we only consider $k = 2, 5, 7$ (Nyerere et al., 2014; Sabini et al., 2020). Computing the nonzero second order partial derivatives, we have:

$$\frac{\partial^2 f_2}{\partial x_1 \partial x_2} = \psi_H, \frac{\partial^2 f_2}{\partial x_1 \partial x_5} = \psi_C, \frac{\partial^2 f_2}{\partial x_1 \partial x_7} = \psi_E, \frac{\partial^2 f_5}{\partial x_4 \partial x_5} = \rho_C \text{ and } \frac{\partial^2 f_5}{\partial x_4 \partial x_7} = \rho_E^*.$$

From (15), it follows that

$$c_1 = v_2 \sum_{i,j=1}^{n} w_i w_j \frac{\partial^2 f_2}{\partial x_i \partial x_j} + v_5 \sum_{i,j=1}^{n} w_i w_j \frac{\partial^2 f_5}{\partial x_i \partial x_j} + v_7 \sum_{i,j=1}^{n} w_i w_j \frac{\partial^2 f_7}{\partial x_i \partial x_j}, \tag{18}$$

which leads to

$$c_1 = \frac{m(\Lambda_C - z)(b - d_1)(a_1 - a_2)a_3 + y\beta_H(\Lambda_H - \mu_H)a_4 a_5}{my\beta_H(\Lambda_C - z)(\Lambda_H - \mu_H)(a - b_1)(b - d_1)^3} v_7 w_7^2, \tag{19}$$

where $a_1 = y(b-d_1)(b_3\beta_H + \phi_1\mu_E) + d_2(y(b_2\beta_H + \beta_C\Lambda_C) + \phi_1 r_H\beta_C)$, $a_2 = (b-d_1)(y\Lambda_H + \phi_1 r_H)\mu_E + b_1 d_2\beta_C$, $a_3 = (b-d_1)(\mu_E\psi_H + \beta_H\psi_E) + d_2(\beta_H\psi_C - \beta_C\psi_H)$, $a_4 = d_2(m(b_1-\Lambda_C) - r_C\phi_2)$, and $a_5 = (b_2\beta_H + \beta_C(a-b_1))(d_2\rho_C + \rho_E^*(b-d_1))$.

$c_1 > 0$ iff

$$(\Lambda_C - z)(\Lambda_H - \mu_H)(a-b_1)(b-d_1)^3 > 0 \text{ and } m(\Lambda_C - z)(b-d_1)(a_1-a_2)a_3 + y\beta_H(\Lambda_H - \mu_H)a_4a_5 > 0. \tag{20}$$

On the other hand, the value of $c_2$ is given by

$$c_2 = v_5w_7\frac{\partial^2 f_5}{\partial x_7\partial\rho_E^*} = \frac{(b_2\beta_H + \beta_c(a-b_1))\Lambda_C N_C^0}{(a-b_1)(b-d_1)z}v_7w_7. \tag{21}$$

$c_2 > 0$ iff the following conditions hold

$$a - b_1 > 0 \text{ and } b - d_1 > 0. \tag{22}$$

Based on the computation of $c_1$ and $c_2$, we can set the following result.

**Theorem 2.** *If the inequalities (20) and (22) hold, the model system (3) undergoes backward bifurcation at* $\mathbb{R}_0 = 1$.

### 2.7. The global stability of the disease free equilibrium ($\mathbb{T}^0$)

**Theorem 3.** *The cryptosporidiosis disease free equilibrium,* $\mathbb{T}^0$*, of the model system (3), is globally asymptotically stable when* $\mathbb{R}_0 < 1$.

**Proof.** The approach in Chavez et al. (2002) is employed to examine the global stability of the disease free equilibrium. Let $X_m, X_n$ and $X_{DFE}$ denote vectors for non-transmitting compartments, transmitting compartments and disease free equilibrium point, respectively, then the model system (3) can be given in the form:

$$\begin{aligned}\frac{dX_m}{dt} &= A_0(X_m - X_{DFE}) + A_1X_n,\\ \frac{dX_n}{dt} &= A_2X_n,\end{aligned} \tag{23}$$

where $A_0, A_1$ and $A_2$ are the matrices to be computed. The cryptosporidiosis disease free equilibrium $\mathbb{T}^0$ is globally asymptotically stable if eigenvalues of $A_0$ are real and negative and $A_2$ is a Metzler matrix (Nyerere et al., 2020; Stephano et al., 2022). A matrix $A = (a_{mn})$ is said to be a Metzler matrix if its off-diagonal elements are non-negative, that is, $a_{mn} \geqslant 0, \forall m \neq n$. In equation (23), we have

$$A_0 = \begin{pmatrix} -\mu_H & \phi_H & 0 & 0\\ 0 & -y & 0 & 0\\ 0 & 0 & -z & \phi_C\\ 0 & 0 & 0 & -m\end{pmatrix},\ A_1 = \begin{pmatrix} -\psi_H & -\psi_C & -\psi_E\\ r_H & 0 & 0\\ 0 & -\rho_C & -\rho_E\\ 0 & r_C & 0\end{pmatrix} \text{ and}$$

$$A_2 = \begin{pmatrix} -(a-b_1) & \psi_C S_H^0 & \psi_E S_H^0\\ 0 & -(b-d_1) & \rho_E S_C^0\\ \beta_H & \beta_C & -\mu_E\end{pmatrix}.$$

Matrix $A_0$ has real and negative eigenvalues whereas $A_2$ is a Metzler matrix if (22) holds. Therefore the cryptosporidiosis disease free equilibrium $\mathbb{T}^0$ is globally asymptotically stable. □

### 2.8. The global stability of the endemic equilibrium ($\mathbb{T}^*$)

.

**Theorem 4.** *The endemic equilibrium*($\mathbb{T}^*$)*is globally asymptotically stable if* $\mathscr{R}_0 > 1$.

**Proof.** We use the method in Osman et al. (2020) for proving the global stability of endemic equilibrium ($\mathbb{T}^*$). Consider the Lyapunov function defined by

$$\begin{aligned}W =& S_H - S_H^* - S_H^*\ln\frac{S_H}{S_H^*} + I_H - I_H^* - I_H^*\ln\frac{I_H}{I_H^*} + R_H - R_H^* - R_H^*\ln\frac{R_H}{R_H^*} + S_C - S_C^* - S_C^*\ln\frac{S_C}{S_C^*} + I_C - I_C^* - I_C^*\ln\frac{I_C}{I_C^*} + R_C - R_C^* - R_C^*\ln\frac{R_C}{R_C^*} + E_V\\ & - E_V^* - E_V^*\ln\frac{E_V}{E_V^*}.\end{aligned} \tag{24}$$

The time derivative of $W$ gives

**Table 4**
State transitions and rates for the CTMC cryptosporidiosis model.

| Event | Transition, $\triangle\mathbf{Z}(t)$ | Transition rate, $p$ |
|---|---|---|
| Recruitment of $S_H$ | $(1,0,0,0,0,0,0)$ | $\Lambda_H N_H$ |
| Immunity lose of $R_H$ | $(1,0,-1,0,0,0,0)$ | $\phi_H R_H$ |
| Human infection from $I_H$ | $(-1,1,0,0,0,0,0)$ | $\psi_H I_H S_H$ |
| Human infection from $I_C$ | $(-1,1,0,0,0,0,0)$ | $\psi_C I_C S_H$ |
| Human infection from $E_V$ | $(-1,1,0,0,0,0,0)$ | $\psi_H E_V S_H$ |
| Natural mortality of $S_H$ | $(-1,0,0,0,0,0,0)$ | $\mu_H S_H$ |
| Recovery of $I_H$ | $(0,-1,1,0,0,0,0)$ | $r_H I_H$ |
| Natural mortality of $I_H$ | $(0,-1,0,0,0,0,0)$ | $\mu_H I_H$ |
| Disease induced mortality of $I_H$ | $(0,-1,0,0,0,0,0)$ | $d_H I_H$ |
| Natural mortality of $R_H$ | $(0,0,-1,0,0,0,0)$ | $\mu_H R_H$ |
| Recruitment of $S_C$ | $(0,0,0,1,0,0,0)$ | $\Lambda_C N_C$ |
| Immunity lose of $R_C$ | $(0,0,0,1,0,-1,0)$ | $\phi_C R_C$ |
| Slaughter of $S_C$ | $(0,0,0,-1,0,0,0)$ | $m_1 S_C$ |
| Cattle infection from $I_C$ | $(0,0,0,-1,1,0,0)$ | $\rho_C I_C S_C$ |
| Cattle infection from $E_V$ | $(0,0,0,-1,1,0,0)$ | $\rho_E E_V S_C$ |
| Natural death of $S_C$ | $(0,0,0,-1,0,0,0)$ | $\mu_C S_C$ |
| Slaughter of $I_C$ | $(0,0,0,0,-1,0,0)$ | $m_2 I_C$ |
| Recovery of $I_C$ | $(0,0,0,0,-1,1,0)$ | $r_C I_C$ |
| Natural death of $I_C$ | $(0,0,0,0,-1,0,0)$ | $\mu_C I_C$ |
| Disease induced death of $I_C$ | $(0,0,0,0,-1,0,0)$ | $d_C I_C$ |
| Natural death of $R_C$ | $(0,0,0,0,0,-1,0)$ | $\mu_C R_C$ |
| Shedding of $E_V$ by $I_S$ | $(0,0,0,0,0,0,1)$ | $\beta_H I_H$ |
| Shedding of $E_V$ by $I_C$ | $(0,0,0,0,0,0,1)$ | $\beta_C I_C$ |
| Natural death of $E_V$ | $(0,0,0,0,0,0,-1)$ | $\mu_E E_V$ |

$$\frac{dW}{dt} = \left(1-\frac{S_H^*}{S_H}\right)\frac{dS_H}{dt} + \left(1-\frac{I_H^*}{I_H}\right)\frac{dI_H}{dt} + \left(1-\frac{R_H^*}{R_H}\right)\frac{dR_H}{dt} + \left(1-\frac{S_C^*}{S_C}\right)\frac{dS_C}{dt} + \left(1-\frac{I_C^*}{I_C}\right)\frac{dI_C}{dt} + \left(1-\frac{R_C^*}{R_C}\right)\frac{dR_C}{dt} + \left(1-\frac{E_V^*}{E_V}\right)\frac{dE_V}{dt}. \tag{25}$$

Substituting the equations of model system (3) into (25) and simplify, we obtain

$$\frac{dW}{dt} = \mathbb{X} - \mathbb{Y}, \tag{26}$$

where

$$\begin{aligned}\mathbb{X} &= \Lambda_H N_H + \phi_H R_H + (\psi_H I_H + \psi_C I_C + \psi_E E_V + \mu_H)S_H^* + (\psi_H I_H + \psi_C I_C + \psi_E E_V)S_H \\ &+(\mu_H + d_H + r_H)I_H^* + r_H I_H + (\mu_H + \phi_H)R_H^* + \Lambda_C N_C + \phi_C R_C + (m_1 + \mu_C)S_C^* \\ &+(\rho_C I_C + \rho_E E_V)S_C^* + (\rho_C I_C + \rho_E E_V)S_C + (m_2 + d_C + \mu_C + r_C)I_C^* + r_C I_C \\ &+(\mu_C + \phi_C)R_C^* + \beta_H I_H + \beta_C I_C + \mu_E E_V^*,\end{aligned}$$

$$\begin{aligned}\mathbb{Y} &= (\psi_H I_H + \psi_C I_C + \psi_E E_V + \mu_H)S_H + \frac{\Lambda_H N_H S_H^*}{S_H} + \frac{\phi_H R_H S_H^*}{S_H} + (\mu_H + d_H + r_H)I_H \\ &+\left(\psi_H + \frac{\psi_C I_C}{I_H} + \frac{\psi_E E_C}{I_H}\right)I_H^* S_H + (\mu_H + \phi_H)R_H + \frac{r_H I_H R_H^*}{R_H} + (m_1 + \mu_C)S_C \\ &+(\rho_E E_V + \rho_C I_C)S_C + \frac{\Lambda_C N_C S_C^*}{S_C} + \frac{\phi_C R_C S_C^*}{S_C} + (m_2 + d_C + \mu_C + r_C)I_C + \rho_C I_C^* S_C \\ &+\frac{\rho_E E_V I_C^* S_C}{I_C} + (\mu_C + \phi_C)R_C + \frac{r_C I_C R_C^*}{R_C} + \mu_E E_V + \frac{\beta_H E_V^* I_H}{E_V} + \frac{\beta_C E_V^* I_C}{E_V}.\end{aligned}$$

From Eq. (26), $\frac{dW}{dt} < 0$ if $\mathbb{X} < \mathbb{Y}$ and $\frac{dW}{dt} = 0$ if $\Omega = \Omega^*$. Therefore, the endemic equilibrium $\mathbb{T}^*$ is the largest invariant set in $\Omega$. Thus, as $t \to \infty$, the LaSalle invariant principle (LaSalle, 1976) concludes that, the solution of model system (3) approaches $\mathbb{T}^*$ when $\mathbb{R}_0 > 1$. Hence, $\mathbb{T}^*$ is globally asymptotically stable if $\mathbb{X} < \mathbb{Y}$. □

## 3. Stochastic model

Stochastic models offer details on the probability of the disease outbreak or extinction (Maliyoni et al., 2019). Stochastic models regard the state variables as discrete and time as continuous (Maliyoni et al., 2019) whereas deterministic models consider the state variables and time as continuous. Therefore stochastic models are more realistic as they explain the discrete movement of individuals between classes. In deterministic models, the basic reproduction number $\mathbb{R}_0$ determines whether there will be a disease outbreak or

fade out in the population. Thus in deterministic models, the disease perishes if $\mathbb{R}_0 < 1$ provided that DFE and endemic equilibrium do not co-exist and persists if $\mathbb{R}_0 > 1$ (Chitnis et al., 2008; Lahodny et al., 2015). The stochastic threshold for the CTMC stochastic model and the basic reproduction number $\mathbb{R}_0$ perform the same purpose. However, their distinct aspect is that depending on the number of infectious individuals at the commencement of the disease occurrence, the stochastic threshold demonstrates that there is a probability for the disease to perish even if the stochastic threshold is $> 1$, while the basic reproduction number $\mathbb{R}_0$ indicates that the disease persists when $\mathbb{R}_0 > 1$ (Maliyoni, 2020). We formulate the CTMC stochastic model and employ the multitype branching process to compute the likelihood for cryptosporidiosis outbreak or extinction in the following section.

### 3.1. CTMC stochastic model development

We use the assumptions, parameters and notations from the deterministic model to develop the CTMC stochastic model. Let time $t \in [0, \infty)$ be continuous and $S_H, I_H, R_H, S_C, I_C, R_C$ and $E_V$ be discrete random variables for susceptible humans, infected humans, recovered humans, susceptible cattle, infected cattle, recovered cattle and *Cryptosporidium* oocysts in the environment respectively.

If $\mathbf{Z} = [S_H, I_H, R_H, S_C, I_C, R_C, E_V]^T$ is the associated random vector for all discrete random variables, then we summarize the events and transition rates in Table 4. An increase by 1, no change and a decrease by 1 in state variables from time $t$ to $(t+\triangle t)$ are represented by $+1, 0$ and $-1$, respectively. It is assumed that the CTMC stochastic model is homogeneous in time and satisfies the Markov property (Maliyoni et al., 2019). According to the Markov property, the time from one event to another is exponentially distributed with parameter (Allen, 2010; Lahodny and Allen, 2013; Lahodny et al., 2015; Maliyoni et al., 2017)

$$\Psi(\mathbf{Z}) = (\Lambda_H + \mu_H)N_H + \phi_H R_H + \lambda_H S_H + (d_H + r_H)I_H + (\Lambda_C + \mu_C)N_C + \phi_C R_C + (m_1 + \lambda_C)S_C + (m_2 + d_C + r_C)I_C + \beta_H I_H + \beta_C I_C + \mu_E E_V, \tag{27}$$

where $N_H = S_H + I_H + R_H, N_C = S_C + I_C + R_C$ and parameters $\lambda_H$ and $\lambda_C$ are described in (1) and (2) respectively.

### 3.2. The multitype branching process

The dynamics of the nonlinear CTMC model near the DFE are usually approximated using the multitype branching processes theory (Maliyoni, 2020). The theory helps to compute the likelihood of disease extinction or outbreak. The branching process may either increase exponentially or terminate to zero, provided that there are few infectious at the commencement of the disease occurrence (Allen, 2017). In the multitype branching process, only infectious compartments are considered, and susceptible classes are assumed to be at the DFE, that is $S_H^0 = \Lambda_H N_H^0/\mu_H$ and $S_C^0 = \Lambda_C N_C^0/(m_1 + \mu_C)$ (Maliyoni, 2020). Offspring probability generating functions (pgfs) for the birth (new infection) and death of infective individuals can be defined since births and mortalities are independent, and the multitype branching process is linear at the DFE and homogeneous in time. These offspring pgfs are used in computing probabilities for cryptosporidiosis extinction or outbreak (Lahodny et al., 2015; Maliyoni et al., 2019).

Assume that infective hosts of type $i, I_i$, can produce infective individuals of type $j, I_j$, and the number of offspring generated by an individual of type $i$ does not depend on the offspring generated by either type $i$ or $j \neq i$ (Allen and van den Driessche, 2013; Lahodny and Allen, 2013; Maliyoni et al., 2017). Moreover, the initial susceptible populations are assumed to be large enough such that $S_H(0) \approx N_H(0) = \Lambda_H N_H^0/\mu_H$ and $S_C(0) \approx N_C(0) = \Lambda_C N_C^0/(m_1 + \mu_C)$; and offspring pgf from type $i$ individuals are the same, independent and identically distributed (iid) (Allen and Lahodny, 2012). Define $\{B_{ji}\}_{j=1}^n$ to be the offspring random variables for type $i$ for $i = 1, \ldots, n$ such that $B_{ji}$ is the number of type $j$ offspring generated by type $i$ infective individuals. The probability of a type $i$ infective individual giving birth to $y_j$ individuals of type $j$ is

$$\mathbb{P}_i(y_1, \ldots, y_n) = \text{Prob}\{B_{1i} = y_1, \ldots, B_{ni} = y_n\}. \tag{28}$$

Thus, the offspring pgf $g_i : [0,1]^n \to [0,1]$ for type $i$ individual given that $I_i(0) = 1$ and $I_j(0) = 1, j \neq i$, is provided as (Allen, 2010; Maliyoni, 2020)

$$g_i(u_1, \ldots, u_n) = \sum_{y_n=0}^{\infty} \sum_{y_{n-1}=0}^{\infty} \cdots \sum_{y_1=0}^{\infty} \mathbb{P}_i(y_1, \ldots, y_n) u_1^{y_1} \ldots u_n^{y_n}. \tag{29}$$

The Eq. (29) helps us to compute an $n \times n$ nonnegative and irreducible expectation matrix $\mathbb{M} = [w_{ji}]$ so that $w_{ji}$ is the expected number of type $j$ infective offspring produced by a type $i$ infective individual. We compute the elements $w_{ji}$ by (Lahodny et al., 2015; Maliyoni, 2020)

$$w_{ji} = \frac{\partial g_i}{\partial u_j}\Big|_{\mathbf{u}=\mathbf{1}} < \infty. \tag{30}$$

The size of the spectral radius of expectation matrix $\mathbb{M}, \rho(\mathbb{M})$ determines the disease's invasion or extinction probability. If $\rho(\mathbb{M}) \leqslant 1$, then the disease extinction likelihood is one, that is:

$$\mathbb{P}_0 = \lim_{t \to \infty} \text{Prob}\{\mathbf{I}(t) = \mathbf{0}\} = 1, \tag{31}$$

and there is a positive likelihood for the disease to persevere in human and cattle populations if $\rho(\mathbb{M}) > 1$, that is:

$$\mathbb{P}_0 = \lim_{t\to\infty} \text{Prob}\{\mathbf{I}(t) = \mathbf{0}\} = p_1^{i_1} p_2^{i_2} \ldots p_n^{i_n} < 1, \tag{32}$$

where $p_i \in (0,1)$ is the unique fixed point of the $n$ offspring pgf, $g_i(p_1, p_2, \ldots, p_n) = p_i$ and $i = 1, 2, \ldots, n$ (Lahodny and Allen, 2013; Lahodny et al., 2015; Maliyoni et al., 2017). The probability of disease extinction for type $i$ infective individuals is equal to the value of $p_i$ while the probability of an outbreak is approximately equal to (Maliyoni et al., 2017)

$$1 - \mathbb{P}_0 = 1 - p_1^{i_1} p_2^{i_2} \ldots p_n^{i_n}. \tag{33}$$

*3.2.1. Stochastic threshold for the CTMC model*

The probability generating functions (pgfs) are formulated by applying the multitype branching process to all infectious compartments in the CTMC stochastic model. Let us use Eq. (29) to describe the offspring pgfs for the infective compartments. Initial susceptible human and cattle populations are assumed be to large enough such that at the DFE we have $S_H^0 = \Lambda_H N_H^0/\mu_H$ and $S_C^0 = \Lambda_C N_C^0/(m_1 + \mu_C)$. Therefore, the offspring pgf for $I_H$ provided that $I_H(0) = 1, I_C(0) = 0$, and $E_V(0) = 0$ is:

$$g_1(u_1, u_2, u_3) = \frac{\psi_H S_H^0 u_1^2 + \mu_H + d_H + r_H + \beta_H u_1 u_3}{\psi_H S_H^0 + \mu_H + d_H + r_H + \beta_H}. \tag{34}$$

The term $\psi_H S_H^0/(\psi_H S_H^0 + \mu_H + d_H + r_H + \beta_H)$ is the probability that a susceptible human acquires infection from infectious human and the infectious human does not perish, thus resulting in two infectious humans. The term $\beta_H/(\psi_H S_H^0 + \mu_H + d_H + r_H + \beta_H)$ denotes the probability that the infected human defecates a *Cryptosporidium* oocyst into the environment, but the infected human does not perish, leading to one infected human and one *Cryptosporidium* oocyst in the environment whereas $(\mu_H + d_H + r_H)/(\psi_H S_H^0 + \mu_H + d_H + r_H + \beta_H)$ is the probability that the infected human can perish or recover before infecting other susceptible individuals thus resulting in zero infected human.

The offspring pgf for $I_C$ provided that $I_H(0) = 0, I_C(0) = 1$, and $E_V(0) = 0$ is:

$$g_2(u_1, u_2, u_3) = \frac{\rho_C S_C^0 u_2^2 + m_2 + \mu_C + d_C + r_C + \psi_C S_H^0 u_1 u_2 + \beta_C u_2 u_3}{\rho_C S_C^0 + m_2 + \mu_C + d_C + r_C + \psi_C S_H^0 + \beta_C}. \tag{35}$$

The term $\rho_C S_C^0/(\rho_C S_C^0 + m_2 + \mu_C + d_C + r_C + \psi_C S_H^0 + \beta_C)$ represents the probability that a susceptible cattle contracts infection from an infected cattle and the infected cattle does not perish thus resulting in two infected cattle. The term $\psi_C S_H^0/(\rho_C S_C^0 + m_2 + \mu_C + d_C + r_C + \psi_C S_H^0 + \beta_C)$ represents the probability that an infectious cattle infect a susceptible human and the infectious cattle does not perish thus leading to one infectious human and one infectious cattle. The term $\beta_C/(\rho_C S_C^0 + m_2 + \mu_C + d_C + r_C + \psi_C S_H^0 + \beta_C)$ denotes the probability that the infectious cattle sheds a *Cryptosporidium* oocyst into the environment and the infectious cattle does not perish thus resulting into one infectious cattle and one *Cryptosporidium* oocyst in the environment while the term $(m_2 + \mu_C + d_C + r_C)/(\rho_C S_C^0 + m_2 + \mu_C + d_C + r_C + \psi_C S_H^0 + \beta_C)$ represents the probability that infectious cattle can perish or recover before infecting other susceptible individuals resulting in zero infectious cattle.

The offspring pgf for $E_V$ provided that $I_H(0) = 0, I_C(0) = 0$, and $E_V(0) = 1$ is:

$$g_3(u_1, u_2, u_3) = \frac{\psi_E S_H^0 u_1 u_3 + \rho_E S_C^0 u_2 u_3 + \mu_E}{\psi_E S_H^0 + \rho_E S_C^0 + \mu_E}. \tag{36}$$

The term $\psi_E S_H^0/(\psi_E S_H^0 + \rho_E S_C^0 + \mu_E)$ denotes the probability that a *Cryptosporidium* oocyst infects a susceptible human and *Cryptosporidium* oocyst does not perish thus resulting in one infectious human and one *Cryptosporidium* oocyst. The term $\rho_E S_C^0/(\psi_E S_H^0 + \rho_E S_C^0 + \mu_E)$ represents the probability that a susceptible cattle contracts infection from *Cryptosporidium* oocyst and *Cryptosporidium* oocyst does not perish thus leading to an infected cattle and a *Cryptosporidium* oocyst. The term $\mu_E/(\psi_E S_H^0 + \rho_E S_C^0 + \mu_E)$ is the probability that *Cryptosporidium* oocyst can die before infecting other susceptible individuals leading to zero *Cryptosporidium* oocyst.

Using Eq. (30), the $3 \times 3$ expectation matrix $\mathbb{M}$ is computed at $\mathbf{u} = (u_1, u_2, u_3) = (1, 1, 1)$ to have

$$\mathbb{M} = \left( \begin{array}{ccc} \frac{\partial g_1}{\partial u_1} & \frac{\partial g_2}{\partial u_1} & \frac{\partial g_3}{\partial u_1} \\ \frac{\partial g_1}{\partial u_2} & \frac{\partial g_2}{\partial u_2} & \frac{\partial g_3}{\partial u_2} \\ \frac{\partial g_1}{\partial u_3} & \frac{\partial g_2}{\partial u_3} & \frac{\partial g_3}{\partial u_3} \end{array} \right) \Bigg|_{\mathbf{u}=\mathbf{1}} = \left( \begin{array}{ccc} \frac{N_1}{D_1} & \frac{\psi_C S_H^0}{D_2} & \frac{\psi_E S_H^0}{D_3} \\ 0 & \frac{N_2}{D_2} & \frac{\rho_E S_C^0}{D_3} \\ \frac{\beta_H}{D_1} & \frac{\beta_C}{D_2} & \frac{N_3}{D_3} \end{array} \right), \tag{37}$$

where

$$\begin{aligned} D_1 &= \psi_H S_H^0 + \mu_H + d_H + r_H + \beta_H, \\ D_2 &= \rho_C S_C^0 + m_2 + \mu_C + d_C + r_C + \psi_C S_H^0 + \beta_C, D_3 = \psi_E S_H^0 + \rho_E S_C^0 + \mu_E, \\ N_1 &= 2\psi_H S_H^0 + \beta_H, N_2 = 2\rho_C S_C^0 + \psi_C S_H^0 + \beta_C, \text{ and } N_3 = \psi_E S_H^0 + \rho_E S_C^0. \end{aligned} \tag{38}$$

**Table 5**
Model parameter values (unit: day$^{-1}$).

| Parameter | Initial Value | Source | Estimates |
|---|---|---|---|
| $\Lambda_H$ | 1/18250 | Lambura et al. (2020) | 0.00005556 |
| $\phi_H$ | 0.0502 | Assumed | 0.04998026 |
| $\psi_H$ | 0.0002 | Assumed | 0.00017128 |
| $\psi_C$ | 0.000015 | Assumed | 0.00001464 |
| $\psi_E$ | 0.00023 | Assumed | 0.00026640 |
| $\mu_H$ | 0.00004 | Zhao et al. (2021) | 0.00003826 |
| $d_H$ | 0.00003 | Assumed | 0.00002855 |
| $r_H$ | 0.07 | Okosun et al., (2016) | 0.07042289 |
| $\Lambda_C$ | 0.3/365 | Nyerere et al. (2019) | 0.00087930 |
| $\phi_C$ | 0.0395 | Assumed | 0.04079650 |
| $m_1$ | 0.235/365 | Mwasunda et al. (2022) | 0.00057135 |
| $\rho_C$ | 0.00015 | Assumed | 0.00010208 |
| $\rho_E$ | 0.00025 | Assumed | 0.00024942 |
| $\mu_C$ | 0.25/365 | Nyerere et al. (2019) | 0.00077155 |
| $m_2$ | 0.00013 | Assumed | 0.00011509 |
| $d_C$ | 0.0002 | Assumed | 0.00017815 |
| $r_C$ | 0.055 | Assumed | 0.05605533 |
| $\beta_H$ | 0.032 | Assumed | 0.03549549 |
| $\beta_C$ | 0.45 | Assumed | 0.52399835 |
| $\mu_E$ | 0.033 | Okosun et al., (2016) | 0.04139149 |

The spectral radius $\rho(\mathbb{M})$ is the stochastic threshold for cryptosporidiosis extinction or persistence in humans and cattle populations. The stochastic threshold $\rho(\mathbb{M})$ and the basic reproduction number $\mathbb{R}_0$ for a stochastic model and deterministic model, respectively, are closely related (Maliyoni et al., 2017). If $\rho(\mathbb{M})\leqslant 1$ or $\mathbb{R}_0\leqslant 1$ then the disease vanishes in human and cattle populations. For the deterministic models, the disease persists in the population if $\mathbb{R}_0 > 1$. Nevertheless, in stochastic models, the disease can vanish or persist even if $\rho(\mathbb{M}) > 1$ based on the present initial size of infectious in a susceptible population (Allen and van den Driessche, 2013; Lahodny and Allen, 2013; Maliyoni, 2020). Hence, if $\rho(\mathbb{M}) > 1$, there exist a fixed point $(p_1, p_2, p_3) \in (0,1)^3$ of the offspring pgfs (34)–(36) that expresses the disease's extinction probability.

Generally, it is not possible to obtain analytical expressions for the extinction probabilities $p_1, p_2$ and $p_3$. However, in some particular cases, the analytical expressions are obtainable (Lahodny et al., 2015). If there are no direct transmissions from human to human, cattle to human and cattle to cattle, we obtain the extinction probabilities $p_1, p_2$ and $p_3$ as follows.

$$\begin{aligned} p_1 &= \frac{a}{a+\beta_H(1-p_3)}, p_2 = \frac{b}{b+\beta_C(1-p_3)}, \\ p_3 &= \frac{z\psi_E\Lambda_H N_H^0 p_1 p_3 + \mu_H\rho_E\Lambda_C N_C^0 p_2 p_3 + z\mu_E\mu_H}{z(\psi_E\Lambda_H N_H^0 + \mu_E\mu_H) + \mu_H\rho_E\Lambda_C N_C^0}. \end{aligned} \tag{39}$$

Solving for $p_3$, we obtain

$$p_3^* = 1, p_3^{**} = \frac{Q_2 - \sqrt{Q_2^2 - 4Q_3}}{2Q_1}, p_3^{***} = \frac{Q_2 + \sqrt{Q_2^2 - 4Q_3}}{2Q_1}, \tag{40}$$

where $Q_1 = \beta_C\beta_H(z(\mu_E\mu_H + \psi_E\Lambda_H N_H^0) + \rho_E\mu_H\Lambda_C N_C^0)$,

$Q_2 = z((a\beta_C + (b+2\beta_C)\beta_H)\mu_E\mu_H + (b+\beta_C)\beta_H\psi_E\Lambda_H N_H^0) + (a+\beta_H)\mu_H\rho_E\beta_C\Lambda_C N_C^0$ and $Q_3 = zQ_1\mu_E\mu_H(a+\beta_H)(b+\beta_C)$. Thus, the fixed points are $(p_1, p_2, p_3) = (1,1,1), (p_1, p_2, p_3^{**})$ and $(p_1, p_2, p_3^{***})$. Therefore, for type $i$ infectious, the probability of disease outbreak is:

$$1 - \mathbb{P}_0 = 1 - p_1^{i_1} p_2^{i_2} p_3^{i_3}, \tag{41}$$

where $i_n$ for $n = 1, 2$ and 3, are the initial values of infected humans, infected cattle and *Cryptosporidium* oocyst introduced into a susceptible population, respectively.

In Section 4.4, the extinction probabilities $p_1, p_2$ and $p_3$ are numerically computed and demonstrate that the approximates for the disease extinction are in good agreement with simulations of the CTMC model.

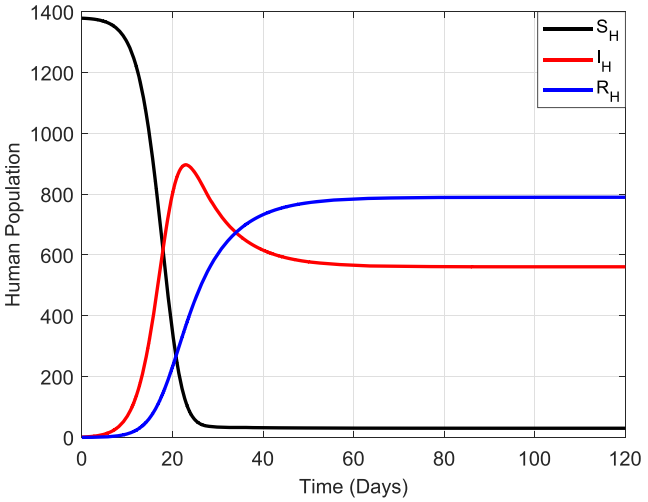


**Fig. 3.** Dynamics of humans, cattle and *Cryptosporidium* oocysts.

## 4. Numerical simulations

Due to limited research in this area, we use the model system (3) to generate data and estimate parameters. The dynamics of the deterministic model and its corresponding CTMC stochastic model are numerically simulated to study cryptosporidiosis in humans and cattle by employing the estimates in Table 5. The multitype branching processes theory is then applied to approximate the likelihood of disease extinction or a major outbreak.

### 4.1. Parameters estimation

The Least Squares Method estimates parameters by minimizing the squared differences between observed data and their expected values. To fit the model to data, we consider the following

$$Y = f(T, \omega) + \epsilon, \tag{42}$$

$$E(Y) = f(T, \omega), \tag{43}$$

where $T$ and $Y$ are independent and dependent variables respectively, $f$ is a linear function, $\omega = (\omega_1, \omega_2, \ldots, \omega_2)$ are the parameters, $\epsilon$ represents noise and $E(Y)$ is the expected value of $Y$. Let $\widehat{\omega}$ be the value of the estimator of $\omega$ that gives the best fit to the data by minimizing $\sum_{j=1}^{k}(y_j - f(t_j, \omega))^2$ (Ndanguza et al., 2020). Data simulation is performed by using Matlab software. The model system (3) is solved numerically using the initial parameter values, as shown in Table 5, then the noise is added to the solution. The noise is normally distributed, that is, $\epsilon \sim \mathcal{N}(Y_i, \sigma^2)$, where $Y_i$ is the output of the model system (3) and $\sigma^2$ is the constant variance which regulates the level of the noise. Once the data set is obtained, we estimate the parameters using the Least Squares Method (Capaldi et al., 2012). Thus, the parameter estimates are presented in Table 5.

### 4.2. Deterministic model

To get insights into the dynamics of cryptosporidiosis, humans, cattle and *Cryptosporidium* oocysts populations are simulated independently. In the presence of cryptosporidiosis, susceptible humans decline to the minimum due to infections. As the susceptible humans diminish, infected humans flourish to maximum and later they decline slightly due to disease mortality and recovery as shown in Fig. 3(a). Susceptible cattle also follow a similar pattern to susceptible humans. Following cryptosporidiosis infection, they decline to the minimum as the number of infected cattle grows before attaining equilibrium. The infected cattle decrease due to disease mortality and recovery. The dynamics of cryptosporidiosis in cattle population is illustrated in Fig. 3(b). As infected humans and cattle defecate into the environment, *Cryptosporidium* oocysts grow and remain constant as shown in Fig. 3(c).

### 4.3. CTMC model simulations

The solutions of deterministic and CTMC stochastic models are graphed together as illustrated in Figs. 4–7. The findings of the deterministic model and its corresponding CTMC stochastic model for cryptosporidiosis in humans and cattle are closely related.

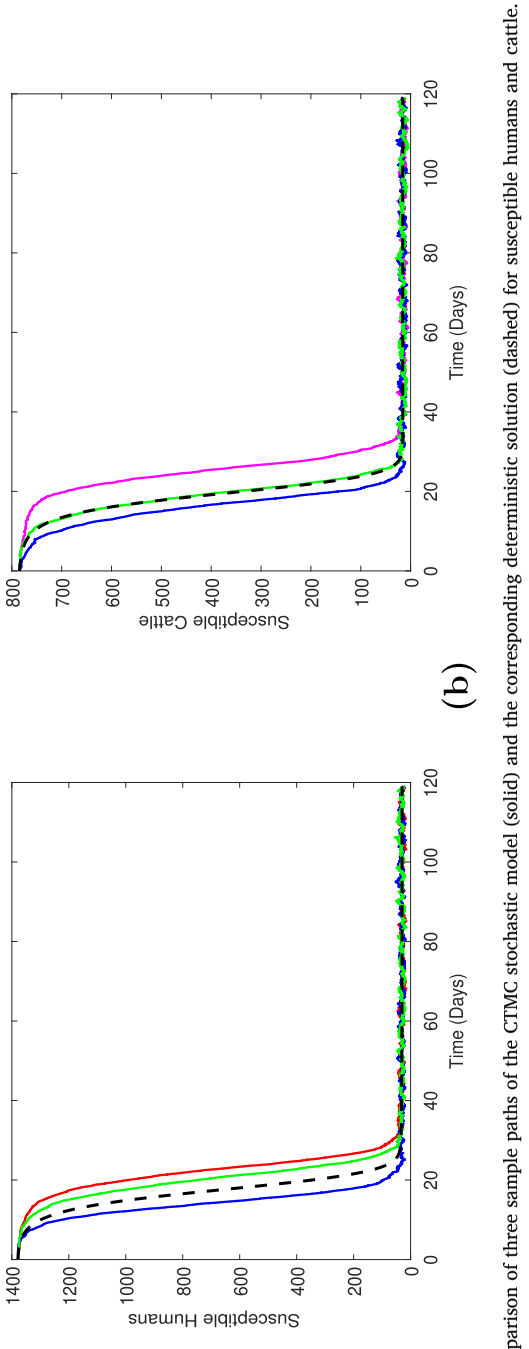


**Fig. 4.** Comparison of three sample paths of the CTMC stochastic model (solid) and the corresponding deterministic solution (dashed) for susceptible humans and cattle.

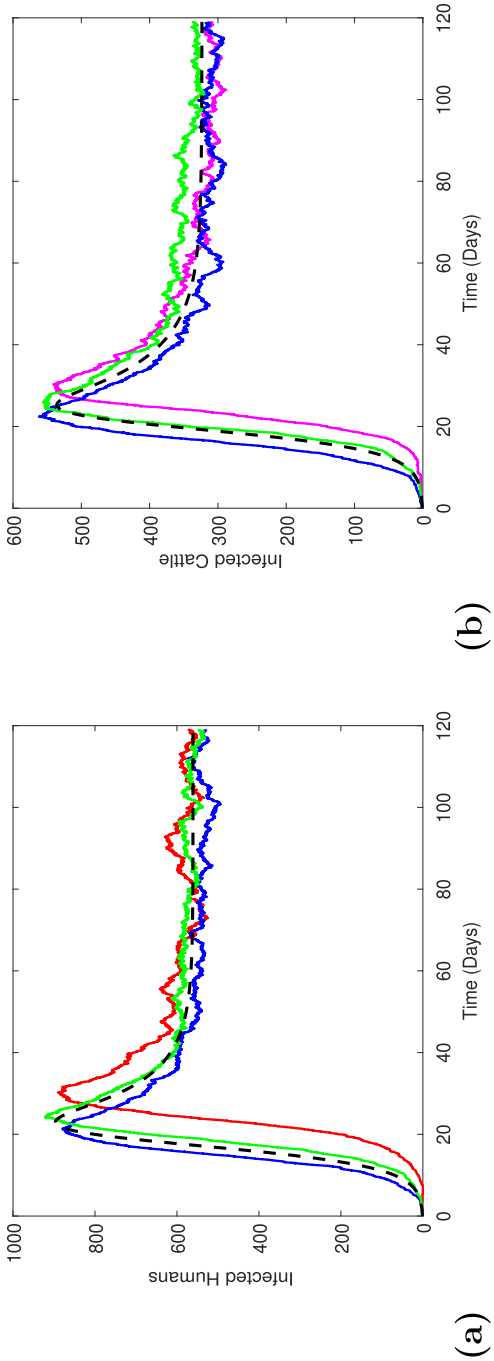


**Fig. 5.** Comparison of three sample paths of the CTMC stochastic model (solid) and the corresponding deterministic solution (dashed) for infected humans and cattle.

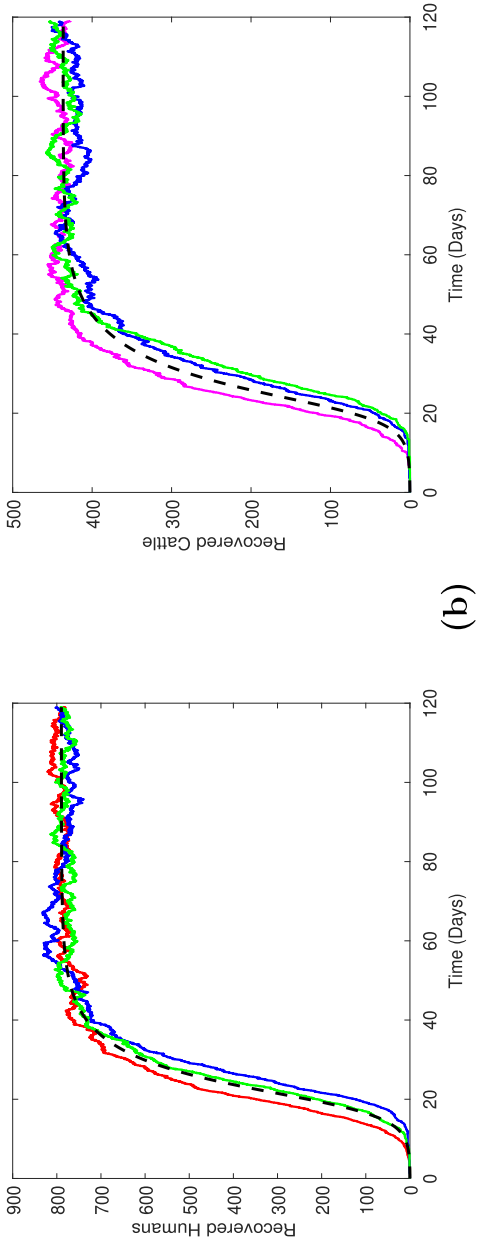


**Fig. 6.** Comparison of three sample paths of the CTMC stochastic model (solid) and the corresponding deterministic solution (dashed) for recovered humans and cattle.

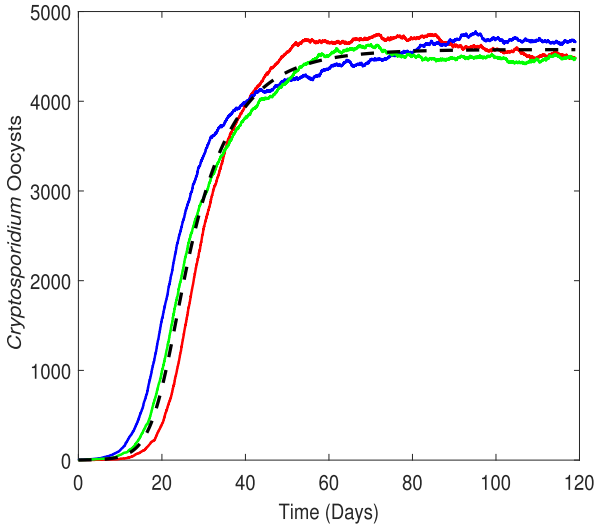


**Fig. 7.** Comparison of three sample paths of the CTMC stochastic model (solid) and the corresponding deterministic solution (dashed) for *Cryptosporidium* oocysts.

**Table 6**
Probability of disease extinction $\mathbb{P}_0$ and numerical approximation $\mathbb{P}_a$.

| $i_{H0}$ | $i_{C0}$ | $e_{V0}$ | $\mathbb{P}_a$ | $\mathbb{P}_0$ |
|---|---|---|---|---|
| 1 | 0 | 0 | 0.6943 | 0.6944 |
| 0 | 1 | 0 | 0.1107 | 0.1109 |
| 0 | 0 | 1 | 0.1261 | 0.1262 |
| 1 | 1 | 0 | 0.0771 | 0.0770 |
| 1 | 0 | 1 | 0.0875 | 0.0876 |
| 0 | 1 | 1 | 0.0141 | 0.0140 |
| 1 | 1 | 1 | 0.0097 | 0.0097 |
| 2 | 0 | 0 | 0.4822 | 0.4822 |
| 0 | 2 | 0 | 0.0122 | 0.0123 |
| 0 | 0 | 2 | 0.0159 | 0.0159 |
| 2 | 2 | 2 | 0.0001 | 0.0001 |

### 4.4. Probability of the disease extinction or outbreak

The multitype branching process fixed point is applied to compute the probability of cryptosporidiosis extinction, $\mathbb{P}_0$, and we compare it to the approximation probability of disease fade out, $\mathbb{P}_a$, determined from a proportion of 10,000 sample paths of the cryptosporidiosis CTMC stochastic model. Table 6 indicates that $\mathbb{P}_a$ and $\mathbb{P}_0$ agree well, where $I_H(0) = i_{H0}, I_C(0) = i_{C0}$ and $E_V(0) = e_{V0}$ are initial conditions. The fixed point in $(0,1)^3$ is given by $(p_1, p_2, p_3) = (0.6944, 0.1109, 0.1262)$.

Fig. 8 provides graphical illustrations for approximated probabilities. It demonstrates that some sample paths go to zero, showing that depending on the initial number of infectious at the onset of the disease, cryptosporidiosis in humans and cattle may fade out even though $\mathbb{R}_0 = 47.9057 > 1$ and $\rho(\mathbb{M}) = 1.5498 > 1$. Using estimate parameter values from Table 5 and altering the initial population for the infective compartments, the approximated probability of the disease extinction $\mathbb{P}_a$ are computed by determining the proportion of sample paths that go to zero before the commencement of the disease.

The initial size of the infected population determines the dynamics of cryptosporidiosis in humans and cattle, as shown in Table 6. Thus, even though the stochastic threshold $\rho(\mathbb{M}) > 1$, cryptosporidiosis in humans and cattle may vanish or persist. Contrarily, the deterministic model demonstrates that the disease is often prevalent provided that $\mathbb{R}_0 > 1$, independent of the initial number of infectious at the onset of cryptosporidiosis. The results in Table 6 reveal that $\mathbb{P}_a$ and $\mathbb{P}_0$ are equal when there is one infective in each infected compartment, two human infectives, two *Cryptosporidium* oocysts and when there are two infectives in each infected compartment. The probability of cryptosporidiosis extinction is higher if it arises from an infected human. However, the likelihood of disease extinction decreases as the number of infected humans increases. On the other hand, the probability of disease major outbreak occurs if the disease is introduced either by an infected cattle or *Cryptosporidium* oocyst or if cryptosporidiosis is emerged from either infected human and infected cattle or infected human and *Cryptosporidium* oocyst or infected cattle and *Cryptosporidium* oocyst or all infectious classes. The probability of disease outbreak is very high if cryptosporidiosis is emerged from all infected classes, and the situation worsens if the number of infectives increases as shown in Table 6. The infected cattle play an important role because they shed a massive amount of *Cryptosporidium* oocysts in the environment (Hatam-Nahavandi et al., 2019; Mtambo et al., 2000). Therefore,

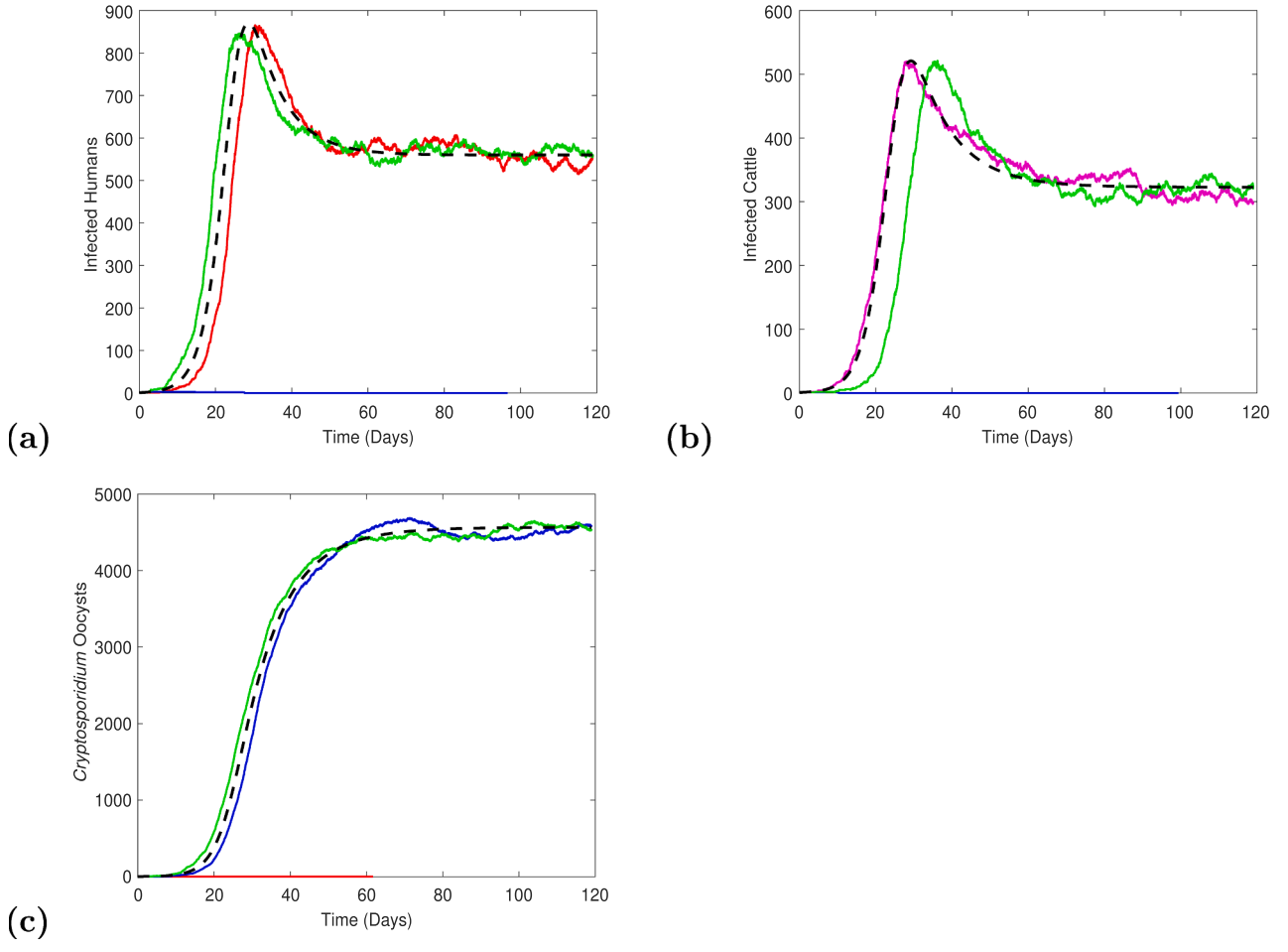


**Fig. 8.** Comparison of three sample paths of the CTMC stochastic model (solid) for infectious classes and the corresponding deterministic solution (dashed).

the control measures should focus on reducing the number of infected humans and cattle, and the number of *Cryptosporidium* oocysts in the environment.

## 5. Conclusion

Deterministic and CTMC stochastic models have been developed and analyzed to examine the dynamics of cryptosporidiosis in humans and cattle. The disease threshold $\mathbb{R}_0$ and its corresponding stochastic threshold $\rho(\mathbb{M})$ that determine the condition for extinction or outbreak of cryptosporidiosis are computed by the next generation matrix method and multitype branching process, respectively. Cryptosporidiosis vanishes if $\mathbb{R}_0 < 1$ and $\rho(\mathbb{M}) < 1$. Though cryptosporidiosis exists in humans and cattle if $\mathbb{R}_0 > 1$, there are chances of a disease major outbreak or extinction when $\rho(\mathbb{M}) > 1$, depending on the initial number of infected individuals that was introduced into the susceptible population.

The analysis of a deterministic model shows that disease free and endemic equilibria exist, and there is a possibility for the model system (3) to undergo backward bifurcation. The sensitivity analysis results show that cattle drive cryptosporidiosis dynamics as they play a great role in shedding *Cryptosporidium* oocysts in the environment. Simulation findings show that the probability of cryptosporidiosis extinction is higher if it arises from an infected human, and there is a high likelihood of disease outbreak if it arises from an infected cattle or from *Cryptosporidium* oocyst or from all three infectious compartments. Therefore, to control cryptosporidiosis, more efforts should be directed to maintaining personal and cattle farm hygiene and decontaminating the environment to kill *Cryptosporidium* oocysts.

## Declaration of Competing Interest

The authors declare that they have no known competing financial interests or personal relationships that could have appeared to influence the work reported in this paper.

## Acknowledgment

The authors acknowledge the University of Dar es Salaam (MUCE) for funding PhD studies.

## References

Aldeyarbi, H.M., El-Ezz, N.M.A., Karanis, P., 2016. Cryptosporidium and cryptosporidiosis: the African perspective. Environ. Sci. Pollut. Res. 23 (14), 13811–13821.
Allen, L.J., 2010. An introduction to stochastic processes with applications to biology. CRC Press.
Allen, L.J., 2017. A primer on stochastic epidemic models: Formulation, numerical simulation, and analysis. Infect. Dis. Modell. 2 (2), 128–142.
Allen, L.J., Lahodny Jr, G.E., 2012. Extinction thresholds in deterministic and stochastic epidemic models. J. Biol. Dyn. 6 (2), 590–611.
Allen, L.J., van den Driessche, P., 2013. Relations between deterministic and stochastic thresholds for disease extinction in continuous-and discrete-time infectious disease models. Math. Biosci. 243 (1), 99–108.
Capaldi, A., Behrend, S., Berman, B., Smith, J., Wright, J., Lloyd, A.L., 2012. Parameter estimation and uncertainty quantication for an epidemic model. Math. Biosci. Eng. 9 (3), 553–576.
Castillo-Chavez, C., Song, B., 2004. Dynamical models of tuberculosis and their applications. Math. Biosci. Eng. 1 (2), 361.
Castro-Hermida, J.A., Almeida, A., González-Warleta, M., Correia da Costa, J.M., Rumbo-Lorenzo, C., Mezo, M., 2007. Occurrence of cryptosporidium parvum and giardia duodenalis in healthy adult domestic ruminants. Parasitol. Res. 101 (5), 1443–1448.
Centers for Disease Control and Prevention, 2020. Parasites - Cryptosporidium (also known as Crypto).https://www.cdc.gov/parasites/crypto/illness.html. Online; accessed 15 December 2020.
Chavez, C.C., Feng, Z., Huang, W., 2002. On the computation of R_0) and its role on global stability. Math. Approach. Emerg Re-emerg. Infect. Dis.: Introduct. 125, 31–65.
Chitnis, N., Hyman, J.M., Cushing, J.M., 2008. Determining important parameters in the spread of malaria through the sensitivity analysis of a mathematical model. Bull. Math. Biol. 70 (5), 1272–1296.
Desai, N.T., Sarkar, R., Kang, G., 2012. Cryptosporidiosis: An under-recognized public health problem. Trop. Parasitol. 2 (2), 91–98.
Diekmann, O., Heesterbeek, J.A.P., Metz, J.A., 1990. On the definition and the computation of the basic reproduction ratio R_0) in models for infectious diseases in heterogeneous populations. J. Math. Biol. 28 (4), 365–382.
Gong, C., Cao, X.-F., Deng, L., Li, W., Huang, X.-M., Lan, F., Zhang, Y., et al., 2017. Epidemiology of cryptosporidium infection in cattle in china: A review. Parasite 2017 (24), 1. https://doi.org/10.1051/parasite/2017001.
Hatam-Nahavandi, K., Ahmadpour, E., Carmena, D., Spotin, A., Bangoura, B., Xiao, L., 2019. Cryptosporidium infections in terrestrial ungulates with focus on livestock: A systematic review and meta-analysis. Parasites Vectors 12 (1), 1–23.
Ibrahim, M., Abdel-Ghany, A., Abdel-Latef, G., Abdel-Aziz, S., Aboelhadid, S., 2016. Epidemiology and public health significance of cryptosporidium isolated from cattle, buffaloes, and humans in egypt. Parasitol. Res. 115 (6), 2439–2448.
Ikiroma, I.A., Pollock, K.G., 2021. Influence of weather and climate on cryptosporidiosis - A review. Zoonoses Public Health 68 (4), 285–298.
Innes, E.A., Chalmers, R.M., Wells, B., Pawlowic, M.C., 2020. A one health approach to tackle cryptosporidiosis. Trends Parasitol. 36 (3), 290–303.
Kahuru, J., Luboobi, L., Nkansah-Gyekye, Y., 2017. Stability analysis of the dynamics of tungiasis transmission in endemic areas. Asian J. Math. Appl. 2017, 1–24.
Lahodny, G.E., Allen, L.J., 2013. Probability of a disease outbreak in stochastic multipatch epidemic models. Bull. Math. Biol. 75 (7), 1157–1180.
Lahodny Jr, G., Gautam, R., Ivanek, R., 2015. Estimating the probability of an extinction or major outbreak for an environmentally transmitted infectious disease. J. Biol. Dyn. 9 (sup1), 128–155.
Lambura, A.G., Mwanga, G.G., Luboobi, L., Kuznetsov, D., 2020. Mathematical model for optimal control of soil-transmitted helminth infection. Comput. Math. Methods Med. 2020.
LaSalle, J.P., 1976. The stability of dynamical systems, vol. 25. SIAM.
Lombardelli, J.A., Tomazic, M.L., Schnittger, L., Tiranti, K.I., 2019. Prevalence of cryptosporidium parvum in dairy calves and gp60 subtyping of diarrheic calves in central argentina. Parasitol. Res. 118 (7), 2079–2086.
Maliyoni, M., 2020. Probability of disease extinction or outbreak in a stochastic epidemic model for west nile virus dynamics in birds. Acta. Biotheor. 69 (2), 91–116.
Maliyoni, M., Chirove, F., Gaff, H.D., Govinder, K.S., 2017. A stochastic tick-borne disease model: Exploring the probability of pathogen persistence. Bull. Math. Biol. 79 (9), 1999–2021.

Maliyoni, M., Chirove, F., Gaff, H.D., Govinder, K.S., 2019. A stochastic epidemic model for the dynamics of two pathogens in a single tick population. Theor. Popul. Biol. 127, 75–90.
Moawad, H.S.F., Hegab, M.H.A.E.-H., Badawey, M.S.R., Ashoush, S.E., Ibrahim, S.M., Ali, A.A.E.-L.S., 2021. Assessment of chitosan nanoparticles in improving the efficacy of nitazoxanide on cryptosporidiosis in immunosuppressed and immunocompetent murine models. J. Parasit. Dis. 45 (3), 606–619.
Mtambo, M., Mpelumbe-Ngeleja, C., Maeda, G., Karimuribo, E., Kusiluka, L., Matovelo, J., Kambarage, D., 2000. Cryptosporidium infection in animals and humans in Tanzania: A review. In: Proceedings of the First University-wide Scientific Conference, 5th–7th April, vol. 4. Sokoine University of Agriculture, Morogoro, pp. 630–642.
Mwasunda, J.A., Irunde, J.I., Kajunguri, D., Kuznetsov, D., 2022. Outbreak or extinction of bovine cysticercosis and human taeniasis: A stochastic modelling approach. Appl. Math. Model. 106, 73–85.
Ndanguza, D., Nyirahabinshuti, A., Sibosiko, C., 2020. Modeling the effects of toxic wastes on population dynamics. Alex. Eng. J. 59 (4), 2713–2723.
Nguyen, S.T., Nguyen, D.T., Le, D.Q., Le Hua, L.N., Van Nguyen, T., Honma, H., Nakai, Y., 2007. Prevalence and first genetic identification of cryptosporidium spp. in cattle in central viet nam. Vet. Parasitol. 150 (4), 357–361.
Nyerere, N., Luboobi, L., Nkansah-Gyekye, Y., 2014. Bifurcation and stability analysis of the dynamics of tuberculosis model incorporating, vaccination, screening and treatment. Commun. Math. Biol. Neurosci. 2014. Article–ID.
Nyerere, N., Luboobi, L.S., Mpeshe, S.C., Shirima, G.M., 2019. Mathematical model for the infectiology of brucellosis with some control strategies. New Trends Math. Sci. 4, 387–405.
Nyerere, N., Luboobi, L.S., Mpeshe, S.C., Shirima, G.M., 2020. Mathematical model for brucellosis transmission dynamics in livestock and human populations. Commun. Math. Biol. Neurosci. 2020 (3), 1–29.
Ogunlade, S., Okosun, K., Lebelo, R., Mukamuri, M., 2016. Optimal control analysis of cryptosporidiosis disease. Glob. J. Pure Appl. Math. 12 (6), 4959–4989.
Okosun, K., Khan, M., Bonyah, E., Ogunlade, S., 2017. On the dynamics of HIV-AIDS and cryptosporidiosis. Eur. Phys. J. Plus 132 (8), 1–25.
Okosun, K., Mukamuri, M., Makinde, O.D., 2016a. Co-dynamics of trypanosomiasis and cryptosporidiosis. Appl. Math. Inform. Sci. 10 (6), 2137–2161.
Osman, S., Otoo, D., Sebil, C., 2020. Analysis of listeriosis transmission dynamics with optimal control. Appl. Math. 11 (7), 712–737.
Ouakli, N., Belkhiri, A., de Lucio, A., Köster, P.C., Djoudi, M., Dadda, A., Khelef, D., Kaidi, R., Carmena, D., 2018. Cryptosporidium-associated diarrhoea in neonatal calves in algeria. Vet. Parasitol.: Reg. Stud. Rep. 12, 78–84.
Pal, M., Bulcha, M., Lema, A., et al., 2021. Cryptospordiosis: An infectious emerging protozoan zoonosis of public health significance. MOJ Biol. Med. 6 (4), 161–163.
Pumipuntu, N., Piratae, S., 2018. Cryptosporidiosis: A zoonotic disease concern. Vet. World 11 (5), 681.
Ramirez, N.E., Ward, L.A., Sreevatsan, S., 2004. A review of the biology and epidemiology of cryptosporidiosis in humans and animals. Microbes Infect. 6 (8), 773–785.
Robertson, L.J., Björkman, C., Axén, C., Fayer, R., 2014. Cryptosporidiosis in farmed animals. In: Cryptosporidium: parasite and disease. Springer, pp. 149–235.
Rossle, N.F., Latif, B., 2013. Cryptosporidiosis as threatening health problem: A review. Asian Pac. J. Trop. Biomed. 3 (11), 916–924.
Ryan, U., Zahedi, A., Paparini, A., 2016. Cryptosporidium in humans and animals-a one health approach to prophylaxis. Parasite Immunol. 38 (9), 535–547.
Scott, C., Smith, H., Mtambo, M., Gibbs, H., 1995. An epidemiological study of cryptosporidium parvum in two herds of adult beef cattle. Vet. Parasitol. 57 (4), 277–288.
Shahiduzzaman, M., Daugschies, A., 2012. Therapy and prevention of cryptosporidiosis in animals. Vet. Parasitol. 188 (3–4), 203–214.
Shaw, H.J., Innes, E.A., Morrison, L.J., Katzer, F., Wells, B., 2020. Long-term production effects of clinical cryptosporidiosis in neonatal calves. Int. J. Parasitol. 50 (5), 371–376.
Shirima Sabini, T., Ismail Irunde, J., Kuznetsov, D., 2020. Modeling the transmission dynamics of bovine tuberculosis. Int. J. Math. Math. Sci. 2020.
Siddique, F., Abbas, R.Z., Babar, W., Mahmood, M.S., Iqbal, A., 2021. Section a: Parasitic diseases cryptosporidiosis. Vet. Pathobiol. Public Health 63–75.
Sponseller, J.K., Griffiths, J.K., Tzipori, S., 2014. The evolution of respiratory cryptosporidiosis: Evidence for transmission by inhalation. Clin. Microbiol. Rev. 27 (3), 575–586.
Stephano, M.A., Irunde, J.I., Mwasunda, J.A., Chacha, C.S., 2022. A continuous time markov chain model for the dynamics of bovine tuberculosis in humans and cattle. Ricerche mat. 1–27.
Striepen, B., 2013. Parasitic infections: time to tackle cryptosporidiosis. Nature 503 (7475), 189–191.
Sulżyc-Bielicka, V., Kołodziejczyk, L., Jaczewska, S., Bielicki, D., Safranow, K., Bielicki, P., Kładny, J., Rogowski, W., 2018. Colorectal cancer and Cryptosporidium spp. infection. PLoS One 13 (4), e0195834.
Tarekegn, Z.S., Tigabu, Y., Dejene, H., 2021. Cryptosporidium infection in cattle and humans in ethiopia: A systematic review and meta-analysis. Parasite Epidemiol. Control 14, e00219.
Thomson, S., Innes, E.A., Jonsson, N.N., Katzer, F., 2019. Shedding of cryptosporidium in calves and dams: evidence of re-infection and shedding of different gp60 subtypes. Parasitology 146 (11), 1404–1413.
Tomczak, E., McDougal, A.N., White Jr, A.C., 2022. Resolution of cryptosporidiosis in transplant recipients: review of the literature and presentation of a renal transplant patient treated with nitazoxanide, azithromycin, and rifaximin. In: Open Forum Infectious Diseases, vol. 9. Oxford University Press, US, p. ofab610.
Van den Driessche, P., Watmough, J., 2002. Reproduction numbers and sub-threshold endemic equilibria for compartmental models of disease transmission. Math. Biosci. 180 (1–2), 29–48.
Walter, E.M., Charles, M., Elick, O., Manfred, M., Domitila, K., 2021. Prevalence of zoonotic cryptosporidium spp. isolates in Njoro sub-county, Nakuru county, Kenya. African. J. Infect. Dis. 15 (2), 3–9.
Zahedi, A., Ryan, U., 2020. Cryptosporidium–an update with an emphasis on foodborne and waterborne transmission. Res. Vet. Sci. 132, 500–512.
Zakir, S., Tafese, W., Mohamed, A., Desa, G., 2021. Review of cryptosporidiosis in calves, children and HIV/AIDS patients. Healthcare Rev. 2 (1), 1–15.
Zhao, J.-Q., Bonyah, E., Yan, B., Khan, M.A., Okosun, K., Alshahrani, M.Y., Muhammad, T., 2021. A mathematical model for the coinfection of buruli ulcer and cholera. Results Phys. 29, 104746.